Collective light-matter interaction. From Purcell to Dicke.

Alexander N. Poddubny

Weizmann Institute of Science, Rehovot 7610001, Israel

poddubny@weizmann.ac.il

March 1, 2025

Contents

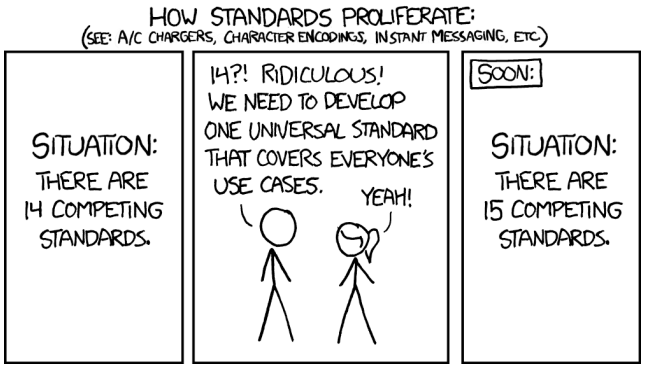

Figure 1.1: xkcd comics #927 on competing standards. Maybe, the same happens for textbooks

of that as well. There are very basic collective interaction effects for X-ray diffraction theory, such as the Borrmann effect of suppression of absorption, that seem to be completely forgotten and have to be rediscovered each time when seen in experiments. The superradiance, collective enhancement of spontaneous emission in emitter arrays, is now seeing a renaissance of research. At the same time, there is not much collaboration between the specialists on various times of emitters, such as real atoms and artificial atoms (quantum dots).

The current book aims to bridge these communities at least partially by considering some basic effects of collective light-matter interactions occurring in various arrays of emitters from a hopefully universal viewpoint. In the first part, I will focus on the linear response regime, that is realized either for very low light intensity (below single photon) or for classical light in the linear optics regime. I will discuss collective enhancement and suppression of the light-matter interaction strength, the difference between strong and weak coupling regimes, Purcell effect, vacuum Rabi splitting. I know there is a little chance of success, as elucidated by the XKCD comic in Fig. 1.1. The whole concept of a textbook might vanish in the age of AI. But I still think it is worth a try. The book does not require knowledge of advanced quantum mechanics or quantum electrodynamics. It is mostly sufficient to know free-space electrodynamics at the undegraduate level.

I am very grateful for multiple discussions and collaborations with many people, in particular with Nir Davidson, Ofer Firstenberg, Johannes Fink, Mikhail Glazov, Eougenius Ivchenko, Yuri Kivshar, Yuri Lozovik, Andrey Miroshnichenko, Alexander Poshakinskiy, Elena Redchenko, Ralf Rohlsberger, Ephraim Shahmoon, Alexandra Sheremet, Jiaming Shi, Andrey Sukhorukov. I thank my family for their constant support.

Chapter 4

Scattering on a single emitter

In this chapter, we consider a most basic problem: interaction of propagating light at a certain frequency ω with the system, having a single optical resonance at the frequency ω_0. The possible setup, corresponding to this model, is schematically illustrated in Fig. 4.1 — it consists of a waveguide, where photons propagate in one dimension either forward or backward, with the constant velocity c, coupled to a two-level atom. However, an actual physical realization can vary. It can involve different types of light emitters in place of the resonant system. For example, as described in the previous chapter, one can consider a plane electromagnetic wave normally incident upon a flat semiconductor quantum well. The equations describing light reflection in such a setup would be the same up to the change of notation.

Before proceeding to the actual calculation, it is important to think what can happen with incoming light wave at the frequency ω depending on the relation ω and the system resonance frequency ω_0. If the light is strong from the resonance, we can expect no interaction. Indeed, due to the energy conservation law, the light can not be absorbed by the emitter. On the other hand, if ω and ω_0 are close, some interaction can take place. The photon can be absorbed, and after that, it can be reemitted back into the waveguide with some probability. As a result, there is a possibility that light can be reflected backward with a certain reflection coefficient r.

Our goal will be to calculate the value of this reflection r depending on the *spectral detuning* $\omega - \omega_0$. By doing this, we will also clarify what is large and what is strong detuning, that it, at which value of $|\omega - \omega_0|$ the reflection can be neglected. Moreover, we will also show that the properties of the system change when it can interact with propagating photons. In fact, our calculation, despite being mostly based on classical Maxwell equations, will allow us to

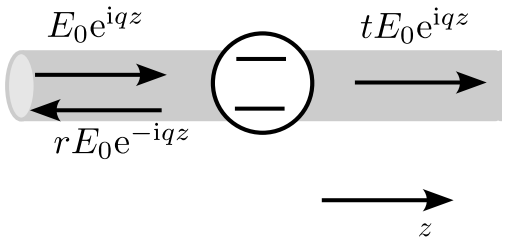

Figure 4.1: Schematics of light reflection and transmission from a resonant scatterer.

find the rate of *spontaneous emission* into the waveguide.

4.1 Brute-force approach

4.1.1 Wave equation

Let us consider a monochromatic electromagnetic wave at the frequency ω, propagating in one direction z at the frequency ω with the velocity c. It then satisfies the usual wave equation

$$\frac{\mathrm{d}^2}{\mathrm{d}z^2}E(z) + q^2 E(z) = 0\,, \tag{4.1}$$

where $q = \omega/c$ is the light wave vector. When writing Eq. (4.1) we do not write explicitly the dependence of the electromagnetic field E on two other spatial coordinates x, y. In the simplest description one can assume $\boldsymbol{E}(x, y, z) = E(z)\boldsymbol{f}(x, y)$, where $\boldsymbol{f}(x, y)$ describes the mode polarization and the spatial distribution in the transverse direction. We assume that those are not affected by the interaction with the emitter, so that transverse and longitudinal degrees of freedom can be separated and it suffices to consider just a single scalar equation (4.1). Now, in order to describe the light interaction with the emitter, we need to introduce external polarization $P(z)$ into the wave equation

$$\frac{\mathrm{d}^2}{\mathrm{d}z^2}E(z) + q^2 E(z) = -4\pi q^2 P(z)\,. \tag{4.2}$$

Here, $P(z)$ is the electromagnetic polarization, induced in the waveguide material, due to the presence of the emitter. By definition, this polarization is in general nonzero within the emitter but quickly vanishes outside. We will now make the next approximation and assume that the emitter is small as compared to other spatial scales in the problem, namely, small as compared

to the light wavelength $\lambda = 2\pi/q$. Then, the polarization can be approximated by a δ-function

$$P(z) = p\delta(z)\,, \tag{4.3}$$

where we introduced the emitter dipole moment p and assumed that the emitter is placed at $z = 0$. The problem is still not quite well defined: we need to specify how to calculate the value of p. Here comes another approximation of the linear response. We say that the emitter dipole moment is nonzero only in the presence of the electric field, and that it is linearly proportional to this electric field, that is

$$p = \alpha E(0)\,, \tag{4.4}$$

where α is the *emitter polarizability* and $E(0)$ is the electromagnetic wave at the position of the emitter $z = 0$. The actual value of α depends on the microscopic properties of an emitter. For example, for an actual atom, it has to be calculated quantum-mechanically. Given α, the system of equations Eqs. (4.1)–(4.4) becomes complete and can be solved analytically.

4.1.2 Emitter polarizability

The goal of this book is to describe the general properties of resonant light-emitter interaction, without going into the microscopic details of the emitter. As such, we can make a following strong assumption about α:

$$\alpha(\omega) = \frac{a}{\omega_0 - \omega - \mathrm{i}\gamma}\,. \tag{4.5}$$

where a and γ are two new real parameters. The parameter a characterizes the strength of the resonance. The γ characterizes the resonance damping because of some other mechanisms, unrelated to the resonant interaction with the photon mode in the waveguide. For example, such term can be related to the spontaneous emission of photons in another optical modes, or it can phenomenologically describe the dephasing because of the interaction with the modes in the environment of the emitter. The perfect emitter corresponds to the limit $\gamma \to +0$. In the simplest quantum mechanical description of a two-level atom, ω_0 corresponds to the energy difference between the levels $|1\rangle$ and $|2\rangle$, $\omega_0 = E_2 - E_1$, and $a = d^2/\hbar$, where d is the matrix element of the atom dipole moment in the direction along the electric field polarization $\boldsymbol{\sigma}$, $d^2 = e2|\langle 1|(\boldsymbol{\sigma}\cdot\boldsymbol{r})|2\rangle|^2$, and e is the electron charge. However, these details depend on the particular type of the emitter and will not be important for the following consideration.

We note, that Eq. (4.5) is valid only in the vicinity of the resonance, for ω close to ω_0. For

large detuning it is necessary to add at least one more *counter-rotating* term,

$$\alpha(\omega) = \frac{a}{\omega_0 - \omega - \mathrm{i}\gamma} + \frac{a}{\omega_0 + \omega + \mathrm{i}\gamma}\,, \tag{4.6}$$

that is maximal at $\omega = -\omega_0 - \mathrm{i}\gamma$. However, we will neglect this term from now on, since we assume $|\omega - \omega_0| \ll \omega, \omega_0$. As an exercise, you can check that Eq. (4.6) satisfies the general Kramers-Kronig relationships for the permittivity.

Solving the wave equation

We are now in position to find light reflection coefficient r and transmission coefficient z. Let assume that an electromagnetic wave with the amplitude E_0 is incident from the left and is scattered on the emitter. Everywhere for $z \neq 0$ the right-hand side of Eq. (4.2) is absent and the solution can be presented as a superposition of right- and left-going plane waves $\exp[\pm \mathrm{i}qz]$. This means that

$$E(z) = \begin{cases} E_0(\mathrm{e}^{\mathrm{i}qz} + r\mathrm{e}^{-\mathrm{i}qz}), & z < 0 \\ E_0 t\mathrm{e}^{\mathrm{i}qz}, & z > 0\,, \end{cases} \tag{4.7}$$

were, r and t are the light reflection and transmission coefficients. In order to find the values of r and t we need to apply the boundary conditions at the emitter position $z = 0$.

The first of these boundary conditons is the continuity of the electric field, $E(-0) = E(+0)$, that yields

$$1 + r = t\,. \tag{4.8}$$

The second of the boundary conditions is obtained by integrating Eq. (4.2) for z from $-\delta z$ to δz around the point $z = 0$ and then setting δz to 0. Since the right-hand side of Eq. (4.2) contains a δ-function, it will not be zero even for $\delta z = 0$. The result yields

$$\frac{\mathrm{d}E}{\mathrm{d}z}\Big|_{z=+0} - \frac{\mathrm{d}E}{\mathrm{d}z}\Big|_{z=-0} = -4\pi q^2 p \tag{4.9}$$

which means that

$$\mathrm{i}q(t + r - 1) = -\frac{4\pi q^2 a}{\omega_0 - \omega - \mathrm{i}\gamma}(1 + r)\,. \tag{4.10}$$

Substituting $t = 1 + r$, we find

$$\mathrm{i}r = -\frac{2\pi qa}{\omega_0 - \omega - \mathrm{i}\gamma}(1 + r) \tag{4.11}$$

which results in

$$r(\omega) = \frac{\mathrm{i}\gamma_{1\mathrm{D}}}{\omega_0 - \omega - \mathrm{i}(\gamma_{1\mathrm{D}} + \gamma)}\,, t(\omega) = \frac{\omega_0 - \omega - \mathrm{i}\gamma}{\omega_0 - \omega - \mathrm{i}(\gamma_{1\mathrm{D}} + \gamma)}\,. \tag{4.12}$$

with

$$\gamma_{1\mathrm{D}} = 2\pi qa\,. \tag{4.13}$$

The total probability that the photon will be reflected or transmitted is given by $|r(\omega)|^2$ and $|t(\omega)|^2$, respectively. We note, that this probabilities do not in general sum up to unity:

$$|r|^2 + |t|^2 = 1 - A, \quad A = \frac{2\gamma\gamma_{1\mathrm{D}}}{(\omega - \omega_0)^2 + (\gamma + \gamma_{1\mathrm{D}})^2}\,. \tag{4.14}$$

Only for $\gamma = 0$ one has $|r|^2 + |t|^2 = 1$, which is the photon flux conservation law. In general, photon can be lost with a probability A. This allows us to better understand the physical sense of the parameter γ: it describes nonradiative losses in the emitter and emission into other photonic modes rather than into the waveguide. Reflection, transmission and absorption spectra $|r(\omega)|^2$, $|t(\omega)|^2$ and $A(\omega)$ are plotted in Fig. 4.2(a).

As expected, away from the resonance one has $r(\omega) \to 0$ and $t(\omega) \to 1$, that is, the system is transparent. At the perfect resonance condition, when $\omega = \omega_0$ and additionally $\gamma = 0$, the probability that photon is transmitted is zero, $t = 0$. At the same time, $r = -1$, that is, the photon will be reflected with 100 % probability and with a π-phase shift. This can be also seen from Fig. 4.2(b), showing real and imaginary parts of r versus ω: for $\gamma/\gamma_{1\mathrm{D}} = 0.1$ the real part almost reaches minus unity at the resonance. The π phase shift originates from the processes of absorption and reemission by the atom.

In order to understand the physical meaning of the parameter $\gamma_{1\mathrm{D}}$ it is instructive to compare Eq. (9.6) with our starting Eq. (4.5). The original equation had a resonance at $\omega = \omega_0 - \mathrm{i}\gamma$, and we now know γ is some damping parameter of the system (see also Appendix B). We will call it the internal decay rate. The reflection coefficient, obtained taking into account the

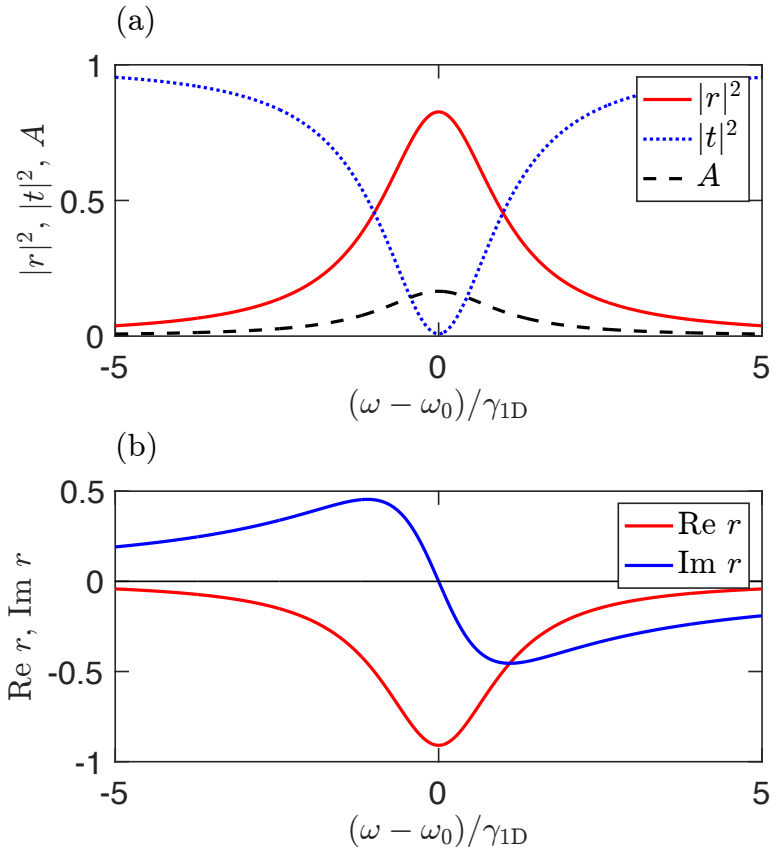

Figure 4.2: (a) Reflection, transmission and absorption spectra for a single resonant emitter. (b) Real and imaginary parts of the reflection spectrum. Calculation has been performed following Eqs. (9.6) for $\gamma/\gamma_{1D} = 0.1$.

system interaction with light, has a resonance at

$$\omega = \omega_0 - \mathrm{i}\gamma - \mathrm{i}\gamma_{1D} \,. \tag{4.15}$$

As such, γ_{1D} can be interpreted as an extra damping rate the emitter acquires due to the interaction with the waveguide photons. It turns out to be the rate of spontaneous radiative decay rate of the emitter into the waveguide. We note, that the expression Eq. (4.13) has been obtained by using an entirely classical electromagnetic calculation. The only quantumness will be encoded in the resonance strength a.

In another words, equation (4.15) can be sought of as the complex resonant frequency of the emitter, renormalized by its interaction with the propagating photons. We note, that in fact γ_{1D} can depend on ω, via the factor $q = \omega/c$ in Eq. (4.13). The parameter a itself can be ω-dependent itself. However, since we are dealing with spectrally narrow resonances, one can

usually neglect this dependence and assume that

$$\gamma_{1D}(\omega) \approx \gamma(\omega_0) = 2\pi\omega_0 a(\omega_0)/c\,. \tag{4.16}$$

This corresponds to the so-called Markovian approximation. It is usually valid when the parameters of the medium surrounding the resonant system slowly vary with frequency on the scale of the resonance linewidth. In the following chapters, we will also consider the situations in which the emitter is strongly coupled to the cavity mode when the Markovian approximation can break down.

4.2 Green function approach

We will now find the same answer in a bit more general way, using the Green function for the Helmholtz equation, We will now use the Green function of the Helmholtz equation,

$$\frac{\mathrm{d}^2G(z,z')}{\mathrm{d}z^2} + q^2G(z,z') = -4\pi q^2\delta(z-z'), G(z,z') = 2\pi\mathrm{i}q\mathrm{e}^{\mathrm{i}q|z-z'|}\,, \tag{4.17}$$

that is derived in Appendix A. Using this Green function, the solution of Eq. (4.2) can be presented as

$$E(z) = E_0\mathrm{e}^{\mathrm{i}qz} - 4\pi q^2\int \mathrm{d}z' G(z,z')P(z') = E_0\mathrm{e}^{\mathrm{i}qz} - 4\pi q^2\int \mathrm{d}z' G(z,z')p\delta(z-z') \tag{4.18}$$

which results in

$$E(z) = E_0\mathrm{e}^{\mathrm{i}qz} + 2\pi\mathrm{i}qp\mathrm{e}^{\mathrm{i}q|z|} \tag{4.19}$$

where the first term in the left-hand side presents the incident wave and the second term is the wave scattered by the emitter. Given Eq. (4.4) and Eq. (4.5) we write

$$(\omega_0 - \mathrm{i}\gamma - \omega)p = aE(0)\,. \tag{4.20}$$

Since $E(0) = E_0 + 2\pi\mathrm{i}qp$, we find

$$(\omega_0 - \mathrm{i}\gamma - \mathrm{i}\gamma_{1D} - \omega)p = aE_0\,, \tag{4.21}$$

where γ_{1D} is the same γ_{1D} as in Eq. (4.13). This equation allows us to find p and after substituting the result into Eq. (4.19) we obtain an electric field

$$E(z) = E_0(\mathrm{e}^{\mathrm{i}qz} + r\mathrm{e}^{\mathrm{i}q|z|}), \quad r = \frac{\mathrm{i}\gamma_{1D}}{\omega_0 - \omega - \mathrm{i}(\gamma + \gamma_{1D})}, \quad p = \frac{aE(0)}{\omega_0 - \omega - \mathrm{i}(\gamma + \gamma_{1D})}\,. \tag{4.22}$$

The answer is exactly equivalent to the one obtained in the previous section. In particular, Eq. (4.21) can be seen as the equation of motion for the emitter under the influence of the driving with the electric field E_0. The complex frequency $\omega_0 - \mathrm{i}\gamma - \mathrm{i}\gamma_{1D}$, entering Eq. (4.21), is the same as (4.15) and it can be seen as the emitter resonance frequency renormalized by the interaction with light.

The advantage of our derivation using the Green function over the derivation in the previous section is that it is much more general. First, we can apply it for emitters interacting with a more complex electromagnetic environment, not just with photons in a waveguide with linear dispersion. In this case we would just need to know the Green function $G(z, z')$, solving for the electromagnetic field in the point z induced by the point dipole z'. Similarly as in this chapter, such Green function can be calculated independently beforehand and does not depend on the properties of the emitters themselves. Equation Eq. (4.21) will then become

$$[\omega_0 - \mathrm{i}\gamma - G(0,0) - \omega]p = aE_0\,, \tag{4.23}$$

where $G(0,0)$ is the field in the origin. Second, Eq. (4.21) can be generalized for an array of N emitters with dipole moments p_m, resonance frequencies $\omega_0^{(m)}$, internal decay rates $\gamma^{(m)}$ and resonance strengths z_m. It will then become a linear system of equations

$$[\omega_0^{(m)} - \mathrm{i}\gamma^{(m)} - \omega]p_m - \sum_{n=1}^{N} G(z_m, z_n)p_n = a_m E_0(z_m)\,. \tag{4.24}$$

If we introduce the matrix $H_{mn} = \delta_{mn}(\omega_{0,m} - \mathrm{i}\gamma) - G(z_m, z_n)$, we can rewrite Eq. (4.24) as

$$\sum_{n=1}^{N} H_{mn}p_n - \omega p_m = a_m E_0(z_m)\,. \tag{4.25}$$

The matrix H_{mn} is a generalization of the complex eigenfrequency Eq. (4.15) to the emitter array. We will extensively study its properties in the following chapters, and we will show that it

can be interpreted as an effective Hamiltonian of the array, interacting with the electromagnetic environment. It is also relatively straightforward to further generalize this equation to a full 3D problem and to include the vector polarization degree of freedom of the emitters.

4.3 Summary

To summarize, in this chapter we have calculated the reflection, transmission and absorption coefficients for light, scattering on a single emitter. We have also calculated the spontaneous decay rate of an emitter into the waveguide modes. This was done in two ways: (a) by directly solving the wave equations with the resonant emitter polarizability and (b) by using the Green function approach. The latter one can be readily generalized for a more complex setting, including $N > 1$ emitters. Such a system will be considered in the next chapter.

4.4 Additional reading

Kramers-Kronig relationships and analytical properties of susceptibility: L. Landau and E. Lifshits, *Statistical physics*, Course of theoretical physics pt. 1 (Butterworth-Heinemann, 1980), SS123.

Light reflection from a quantum well: F. Tassone et al., "Quantum-well reflectivity and exciton-polariton dispersion", Phys. Rev. B **45**, 6023–6030 (1992)

Light reflection from a cavity coupled to the waveguide: M. F. Yanik et al., "Stopping Light in a Waveguide with an All-Optical Analog of Electromagnetically Induced Transparency", Phys. Rev. Lett. **93**, 233903 (2004)

Light reflection from an atom: A. Asenjo-Garcia et al., "Exponential improvement in photon storage fidelities using subradiance and "selective radiance" in atomic arrays", Phys. Rev. X **7**, 031024 (2017)

Chapter 5

Scattering on two emitters

We will now proceed to the next chapter, where we will consider light interaction with N resonant emitters. The fundamental questions to answer are in this chapter are as follows: How to treat the multiple-emitter system? Will the interaction be stronger or weaker than for a single emitter? What will be the spontaneous decay rate of the emitters? Let us start with the illustrative case of $N = 2$ emitters, located at the points $z_1 = 0$ and $z_2 = d$. Already this problem is rich enough to illustrate a lot of basic physics.

Let us first assume that the emitters are characterized by the resonant frequencies $\omega_0^{(1,2)}$, radiative decay rates $\gamma_{1D}^{(1,2)}$, and internal decay rates $\gamma^{(1,2)}$ that all can in general be different. How should we proceed to evaluate, say, light reflection coefficient from both emitters $r_{\rm tot}$? Based on the results in the previous chapter, we could start to decompose electric field between the emitters into plane waves, similar to Eq. (4.7). However, this will be more involved, since we would now have to include 3 regions: leftmost of the first emitter, $z < 0$, between the emitters, $0 < z < d$ and to the right of the second emitter, $z > d$. The electric field will be characterized by four complex amplitudes In total. This amplitude to be determined by the two boundary conditions at each of the emitter position. Such a procedure is quite tractable for a computer but rather cumbersome, especially if one has $N > 2$ emitters. So it is rarely used in practice. We will now present two alternative ways to find the same answer, that are more compact and are easier to generalize for larger N.

5.1 Multiple scattering approach

Following Eqs. (9.6) we can introduce reflection and transmission coefficients $r_{1,2}$, $t_{1,2}$ for each emitter. Then we calculate the reflection coefficient can be calculated as sum of multiple scattering processes as below illustrated Here, three terms correspond to light having bounced

$$r_{\rm tot} = r_1 + t_1^2 r_1 \mathrm{e}^{2\mathrm{i}\varphi} + t_1^2 r_1 r_2 \mathrm{e}^{2\mathrm{i}\varphi} + \ldots$$

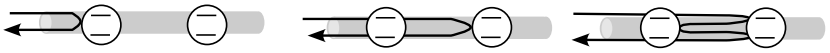

Figure 5.1: Illustration of the geometric series to calculate light reflection coefficient from the two emitters.

zero, once and twice between the emitters, respectively, before being reflected back. At each roundtrip, the reflection amplitude gets a factor $r_1 r_2 \exp(2\mathrm{i}\varphi)$ where $\varphi = \omega d/c$ is the light phase while propagating between the two emitters. As a result, we obtain a geometric series, that can be summed analytically:

$$r_{\rm tot} = r_1 + \frac{t_1^2 r_2 \mathrm{e}^{2\mathrm{i}\varphi}}{1 - r_1 r_2 \mathrm{e}^{2\mathrm{i}\varphi}} \,. \tag{5.1}$$

In a similar fashion one can also obtain a transmission coefficient through both emitters

$$t_{\rm tot} = \frac{t_1 t_2 \mathrm{e}^{\mathrm{i}\varphi}}{1 - r_1 r_2 \mathrm{e}^{2\mathrm{i}\varphi}} \,. \tag{5.2}$$

Interestingly the reflection coefficient Eq. (5.1) is not symmetric with respect to first and second emitter, while the transmission coefficient Eq. (5.2) is symmetric. This is non a coincidence but a result of a general principle of *time-reversal invariance*, also related to *Lorentz reciprocity*. This principle, when applied to our one-dimensional setup, states that while reflection coefficients for light incident from the left and from the right of the structure can be different, the amplitude transmission coefficients from the left to the right and from the right to the left are the same. Swapping the two emitters is equivalent to swapping the direction the light is incident from. Such symmetry holds in the linear optics regime unless an external magnetic field is applied.

The multiple scattering procedure can be, in principle, readily generalized for an arbitrary number of emitters, but it is still slightly inconvenient. Thus, we will consider two more approaches later in this chapter.

Figure 5.2 shows the reflection spectra dependence on the distance between the emitters, encoded by the phase $\varphi = \omega_0 d/c$. It is clear that the distance matters much. For $\varphi = 0, \pi, 2\pi$, corresponding to $d = 0, \lambda_0/2, \lambda_0$ (λ_0 is the light wavelength at the emitter resonance frequency), the spectrum has a single Lorentzian peak. The half-width at half-maximum for this peak is equal to $2\gamma_{1D}$, twice larger than for a single emitter, compare Fig. 4.2(a) and Fig. 5.2(a). For intermediate values of $0 < \varphi < \pi$ the peak is in general asymmetric. The value of $\varphi = \pi/2$ corresponds to a single symmetric peak with significantly lower spectral width than for $\varphi = 0, \pi$. This overall behaviour can be understood from a basic arguments of constructive and destructive interference for light exhibiting multiple scattering events, see Fig. 5.1. For φ being an integer number of π, all the waves going from emitter 1 to emitter 2 and back interfere constructively with each other. Hence, the overall reflection is enhanced as compared to that for one emitter. This is the essence of the collective enhancement effect. For $\varphi = \pi/2$ the interference is desctructive and the reflection is suppressed.

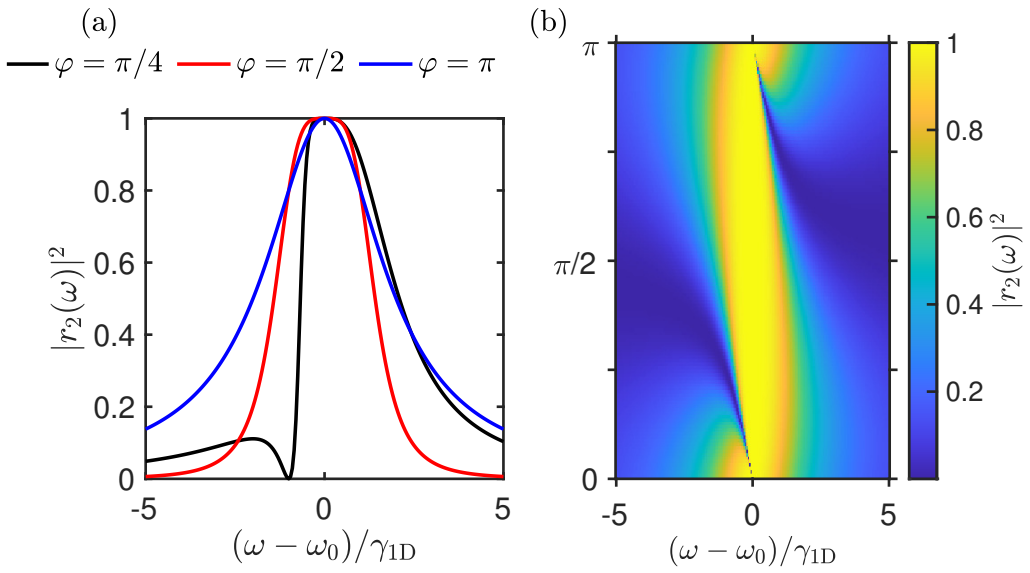

Figure 5.2: Reflection spectra for three specific values of $\varphi = \omega_0 d/c$ and the dependence of the reflection spectra on φ. Calculation has been performed for $\gamma = 0$ and identical emitters.

There are also sharp narrow dips in the reflection spectrum when φ is close to 0 or π, but not exactly equal. To understand them better, in the next chapter we will develop a more involved technique of eigenmode decomposition for the reflection and transmission coefficients.

5.2 Non-Hermitian Hamiltonian method

We will now present in detail the Non-Hermitian Hamiltonian method that was already briefly mentioned in the previous chapter. To this end, we generalize Eqs. (4.2)–(4.4) for our system:

$$\frac{\mathrm{d}^2}{\mathrm{d}z^2}E(z) + q^2 E(z) = -4\pi q^2 \sum_{n=1}^{N} \delta(z - z_n) p_n \,, \tag{5.3}$$

where

$$p_n = \frac{a^{(n)}}{\omega_0^{(n)} - \omega - \mathrm{i}\gamma^{(n)}} E(z_n) \tag{5.4}$$

are the corresponding dipole moments. Similarly to Eq. (4.18) we find

$$E(z) = E_0 \mathrm{e}^{\mathrm{i}qz} + \sum_{n=1}^{N} G(z, z_n) p_n \,, \tag{5.5}$$

Substituting Eq. (5.5) into Eq. (5.4) we obtain

$$\sum_{n=1}^{N} H_{mn} p_n - \omega p_m = a_m E_0 \mathrm{e}^{\mathrm{i}qz_m} \,. \tag{5.6}$$

with

$$\begin{aligned} H_{mn} &= (\omega_0^{(m)} - \mathrm{i}\gamma^{(m)})\delta_{mn} - a_m G(z_m, z_n) \\ &\equiv (\omega_0^{(m)} - \mathrm{i}\gamma^{(m)})\delta_{mn} - \gamma_{1\mathrm{D}}^{(m)} \mathrm{e}^{\mathrm{i}q|z_m - z_n|} \,, \end{aligned} \tag{5.7}$$

being the effective Hamiltonian matrix. We stress, that the matrix Eq. (5.7) is (i) non-Hermitian, (ii) symmetric and (iii) in general depends on the light frequency ω via the wave vector $q = \omega/c$. We will further discuss its properties in the following chapter 5.3.

Now, the dipole moments p_m can be found from the linear system of equations (5.6). It is instructive to introduce the matrix *Green function* of the emitter array, defined as an inverse of the matrix in the left hand-side of (5.6)

$$\mathcal{G}_{mn}(\omega) = \left[\left(H(\omega) - \omega \hat{1} \right)^{-1} \right]_{mn} \tag{5.8}$$

($\hat{1}$ is the $N \times N$ identity matrix) . With the help of the Green function we write

$$p_m = \sum_{n=1}^{N} G_{mn} a_m E_0 \mathrm{e}^{\mathrm{i}qz_m} \,. \tag{5.9}$$

In order to find light reflection and transmission coefficients r_{tot} and t_{tot}, one substitutes Eqs. (5.9) into Eq. (5.5) and takes the limits $z < z_1$ or $z > z_2$, respectively. Thus,

$$E\Big|_{z<z_1} = E_0 \mathrm{e}^{\mathrm{i}qz} + r_{\mathrm{tot}} E_0 \mathrm{e}^{\mathrm{i}qz} \,, \tag{5.10}$$

$$E\Big|_{z>z_2} = t_{\mathrm{tot}} E_0 \mathrm{e}^{\mathrm{i}qz} \,, \tag{5.11}$$

with

$$r_{\mathrm{tot}} = \sum_{n,m=1}^{N} \mathrm{e}^{\mathrm{i}q(z_m+z_n)} \frac{\gamma_{1\mathrm{D}}^{(m)}}{2\pi q} \mathcal{G}_{mn}(\omega), \quad t_{\mathrm{tot}} = 1 + \sum_{n,m=1}^{N} \mathrm{e}^{\mathrm{i}q(z_m-z_n)} \frac{\gamma_{1\mathrm{D}}^{(m)}}{2\pi q} \mathcal{G}_{mn}(\omega) \,. \tag{5.12}$$

Equations (5.12) are valid for arbitrary N. We leave it as an excercise to prove, that for particular case of $N = 2$ they reduce to Eq. (5.1) and Eq. (5.2).

5.3 Complex eigenmodes

As has been mentioned in the previous chapter, the effective non-Hermitian Hamiltonian (5.7) does in general depend on the light frequency. This dependence comes from several places. First, as has been already mentioned in Chapter 4, even the coefficients a, $\gamma_{1\mathrm{D}}$ and γ can depend on ω. Typically, they change much only when ω changes by large value on the order of c/R, where R is the characteristic emitter size. There is an exception of so-called *giant atoms*, that are essentially superconducting qubits with the size on the order of the wavelength. There the $\gamma_{1\mathrm{D}}(\omega)$ dependence is fast [5]. However, usually it is slow and can be neglected. The second place, where H_{mn} depends on ω, is the phase factor $\exp[\mathrm{i}\omega|z_m - z_n|/c] \equiv \exp(\mathrm{i}\omega d/c)$ for the considered case of $N = 2$ emitters . This factor changes when the ω variation is on the order of c/d, that is inverse flight time of light between the two emitters. Typically, for small emitters $\delta z \ll d$, so $c/d \gg c/R$ and the dependence of this factor on ω is more important. Still, due to the large light velocity typically $R/c \ll \gamma_{1\mathrm{D}}$, the flight time is much smaller than the spontaneous emission time. Equivalently, one can say that the scale at which $\exp(\mathrm{i}\omega d/c)$ changes is much larger than the resonance linewidth $\gamma_{1\mathrm{D}}$. For example, for superconducting

qubits coupled to the waveguide one has $\gamma_{1D} \sim 10$ MHz $\times 2\pi$ and $\omega_0 \sim 10$ GHz $\times 2\pi \gg \gamma_{1D}$. Even if the spacing between the qubits is on the order of the light wavelength $\lambda = 2\pi c/\omega_0$ at the qubit resonance frequency, the photon flight time will be on the order of $2\pi/\omega_0$ and much shorter than $2\pi/\gamma_{1D}$, see e.g. Ref. [6]. As such, one can safely neglect the frequency dependence of $\exp(\mathrm{i}\omega d/c)$ and set

$$H_{mn}(\omega) \to H_{mn}(\omega_0)\,, \tag{5.13}$$

where ω_0 is the emitter resonance frequency. By doing this we also assume that the spread of the resonance frequencies is small, $|\omega_0^{(1)} - \omega_0^{(2)}| \ll \omega_0^{(1,2)}$, so it does not matter which exactly ω_0 we choose in Eq. (4.16). Equation (4.16) is termed Markovian approximation. It is very general, and it means that the photon (or general reservoir) dynamics is much faster than the dynamics of the emitters that we are interested in. We will now show that the Markovian approximation considerably simplifies the analysis. Later on, in Sec. 5.6, we will also look beyond this approximation.

Once the Markovian approximation is done, the system Eq. (5.6) can be solved by expanding p_n over the *collective eigenmodes* of the frequency-independent Hamiltonian H_{mn}. There is, however, one important caveat. The Hamiltonian Eq. (5.7) is non-Hermitian, but it is still complex-symmetric. We will introduce the eigenvectors $\psi_n^{(\nu)}$ and eigenfrequencies $\omega^{(\nu)}$ in the conventional way:

$$\sum_{n=1}^{N} H_{mn}\psi_n^{(\nu)} = \omega^{(\nu)}\psi_m^{(\nu)}\,, \tag{5.14}$$

but the caveat will reveal itself in the *unconjugated orthogonality* condition [7]:

$$\sum_{n=1}^{N} \psi_n^{(\nu)}\psi_n^{(\mu)} = \delta_{\mu\nu}\,. \tag{5.15}$$

The condition (5.15) for the Hamiltonian with the property $H_{mn} = H_{nm}$ is different from the usual condition

$$\sum_{n=1}^{N} \psi_n^{(\nu),*}\psi_n^{(\mu)} = \delta_{\mu\nu}\,. \tag{5.16}$$

for the usual Hermitian Hamiltonian , $H_{mn} = H_{nm}^*$. It can be still derived by exactly the same

way. Multiplying Eq. (5.14) by ψ_m^μ and summing over m we find

$$\sum_{n,m=1}^{N} H_{mn}\psi_n^{(\nu)}\psi_n^{(\mu)} = \omega^{(\nu)}\sum_{n=1}^{N}\psi_n^{(\nu)}\psi_n^{(\mu)}\,, \tag{5.17}$$

On the other hand, if we write

$$\sum_{n=1}^{N} H_{mn}\psi_n^{(\nu)} = \omega^{(\nu)}\psi_m^{(\nu)}\,, \tag{5.18}$$

multiply by ψ_m^ν and summing over m we find

$$\sum_{n,m=1}^{N} H_{mn}\psi_n^{(\mu)}\psi_n^{(\nu)} = \omega^{(\mu)}\sum_{n=1}^{N}\psi_n^{(\nu)}\psi_n^{(\mu)}\,. \tag{5.19}$$

Substracting Eq. (5.19) from Eq. (5.17) we find

$$\sum_{n=1}^{N}\psi_n^{(\nu),*}\psi_n^{(\mu)}(\omega^{(\mu)}-\omega^{(\nu)}) = 0\,. \tag{5.20}$$

which leads to Eq. (5.20): the modes are orthogonal once their eigenfrequencies are different.

Given the condition Eq. (5.15) we can expand the solution of Eq. (5.6) in the usual way:

$$p_n = E_0\sum_{\nu=1}^{N}\frac{\psi_n^{(\nu)}\langle\nu|q\rangle}{\omega^{(\nu)}-\omega}, \quad \langle\nu|a|q\rangle \equiv \sum_{n=1}^{N}\psi_n^{(\nu)}a_n e^{iqz_m}\,. \tag{5.21}$$

where we have introduced an unconjugated scalar product notation $\langle\nu|\mu\rangle$ for the left-hand-side of Eq. (5.15) and also for the overlap $\langle\nu|a|q\rangle$ of the incident plane wave $\exp(iqz_m)$ with the mode ν weighted by the emitter radiative decay rates. This allows us to express the reflection and transmission coefficients in terms of eigenmodes. Equations (5.12) then acquire an especially simple form if all decay rates are the same, $\gamma_{1D}^{(m)} \equiv \gamma_{1D}$:

$$r_{\rm tot}(\omega) = i\sum_{\nu=1}^{N}\frac{\gamma_{1D}\langle q|\nu\rangle\langle\nu|q\rangle}{\omega^{(\nu)}-\omega}, \quad t_{\rm tot}(\omega) = 1 + i\sum_{\nu=1}^{N}\frac{\gamma_{1D}\langle -q|\nu\rangle\langle\nu|q\rangle}{\omega^{(\nu)}-\omega}\,. \tag{5.22}$$

The advantage of Eqs. (5.22) is that they clearly show that the reflection and transmission spectra have resonances at the collective eigenmode frequencies. To be more precise, the spectra $|r_{\rm tot}(\omega)|^2, |t_{\rm tot}(\omega)|^2$ will have resonances at ω close to $\mathrm{Re}\,\omega^\nu$ with linewidths of $|\,\mathrm{Im}\,\omega^\nu$.

The states with low $|\operatorname{Im}\omega_\nu|$ will be manifested as sharp resonances.

5.4 Purcell enhancement

Before considering the case of two identical emitters, it is instructive to look closer first into two different emitters, with different resonant frequencies and different values of γ_{1D}. The effective Hamiltonian Eq. (5.7) then becomes

$$H = \begin{pmatrix} \omega_0^{(1)} - \mathrm{i}\gamma_{1D}^{(1)} & -\mathrm{i}\gamma_{1D}\mathrm{e}^{\mathrm{i}\varphi} \\ -\mathrm{i}\gamma_{1D}\mathrm{e}^{\mathrm{i}\varphi} & \omega_0^{(2)} - \mathrm{i}\gamma_{1D}\gamma_{1D}^{(2)} \end{pmatrix} , \tag{5.23}$$

For simplicity we set $\gamma = 0$ in this chapter. Let us assume that the spectral detuning between the two resonance frequencies is large, or, to be more precise,

$$|\omega_0^{(1)} - \omega_0^{(2)} - \mathrm{i}\gamma_{1D}^{(1)} + \mathrm{i}\gamma_{1D}^{(2)}| \gg \gamma_{1D}^{(1,2)} .$$

Then we can expect that the effects of the collective interaction between the two emitters are weak. Formally, this means that the eigenfrequencies of Eq. (5.23) can be found using the second-order quantum mechanical perturbation theory. In particular, the complex resonance frequency of the first emitter, slightly renormalized due to the interaction with the second one, can be written as

$$\tilde{\omega}_0^{(1)} = \omega_0^{(1)} - \mathrm{i}\gamma_{1D}^{(1)} + \frac{\gamma_{1D}^{(1)}\gamma_{1D}^{(2)}\mathrm{e}^{2\mathrm{i}\varphi}}{\omega_0^{(1)} - \omega_0^{(2)} - \mathrm{i}\gamma_{1D}^{(1)} + \mathrm{i}\gamma_{1D}^{(2)}} , \tag{5.24}$$

Equation (5.24) is quite instructive. It tells us that both the radiative decay rate $-\operatorname{Im}\omega$ and the resonance frequency are changed by the interaction. The first effect, radiative correction to the resonance frequency has analogy to the *Lamb shift* in vacuum quantum electrodynamics. The second effect is the correction to the decay rate of the emitter in the presence of another one,

$$\frac{-\operatorname{Im}\tilde{\omega}_0^{(1)}}{\gamma_{1D}^{(1)}} = 1 + \operatorname{Im}\frac{\gamma_{1D}^{(2)}\mathrm{e}^{2\mathrm{i}\varphi}}{\omega_0^{(1)} - \omega_0^{(2)} - \mathrm{i}\gamma_{1D}^{(1)} + \mathrm{i}\gamma_{1D}^{(2)}} \approx 1 + \operatorname{Re}[r_2(\omega_0^{(1)})\mathrm{e}^{2\mathrm{i}\varphi}] \tag{5.25}$$

where

$$r_2(\omega) = \frac{\mathrm{i}\gamma_{1D}^{(2)}}{\omega_0^{(2)} - \omega - \mathrm{i}\gamma_{1D}^{(2)}} . \tag{5.26}$$

is the reflection coefficient of the second emitter. The factor in the right-hand side of Eq. (5.25) is the ratio of the decay rates of the first emitter in the presence of the second one and without

the second one. It can be termed as a generalized *Purcell factor*. In his seminal work [8] Purcell understood that the spontaneous decay rate is different for an emitter in vacuum and in a cavity. Now the term Purcell factor is used to describe the modification of the spontaneous decay rate in any structured electromagnetic environment. In this paragraph, the environment is provided by the second emitter. However, in principle the second part of Eq. (5.24) is valid for emitter near any mirror. For example, in Ref. [9] the authors have measured the modification of the radiative lifetime the presence of a planar dielectric mirror.

The answer Eq. (5.24) can be also recovered without involving the concept of non-Hermitian Hamiltonian, directly from the resonances of the reflection coefficient of the two emitters. The central idea here is that the collective eigenmodes correspond to the complex poles of the collective linear response function, for example, of the reflection or transmission coefficient for the two emitters. We see from Eq. (5.2) that the resonance condition for the reflection or transmission of light through two emitters is given just by

$$1 - r_1 r_2 \exp(2\mathrm{i}\varphi) = 0\,. \tag{5.27}$$

Equation (5.27) is just the usual condition for the Fabry-Pérot resonance in the cavity, made of two mirrors with the reflection coefficients r_1 and r_2. However, if we take into account that in our case the mirrors are resonant, we will also find "for free" the collective eigenmode frequencies. Indeed, if we substitute

$$r_1 = \frac{\mathrm{i}\gamma_{1\mathrm{D}}^{(1)}}{\omega_0^{(1)} - \omega - \mathrm{i}\gamma_{1\mathrm{D}}^{(1)}} \tag{5.28}$$

into Eq. (5.27) and solve for ω for fixed r_2, we recover

$$\omega = \omega_0 - \mathrm{i}\gamma_{1\mathrm{D}}^{(1)}(1 + r_2 \mathrm{e}^{2\mathrm{i}\varphi})\,, \tag{5.29}$$

in exact agreement with Eq. (5.24),Eq. (5.25).

It is also instructive to plot reflection spectra for two unidentical emitters, with $\gamma_{1\mathrm{D}}^{(2)} \gg \gamma_{1\mathrm{D}}^{(1)}$ as function of their spectral detuning $\omega_0^{(1)} - \omega_0^{(2)}$. This is done in Fig. 5.3. Since $\gamma_{1\mathrm{D}}^{(2)} \gg \gamma_{1\mathrm{D}}^{(1)}$, away from the first emitter resonance it does not contribute much to the reflection and one has $r_{\mathrm{tot}} \approx r_2$. Closer to the resonance the presence of the first emitter is manifested as a specrally

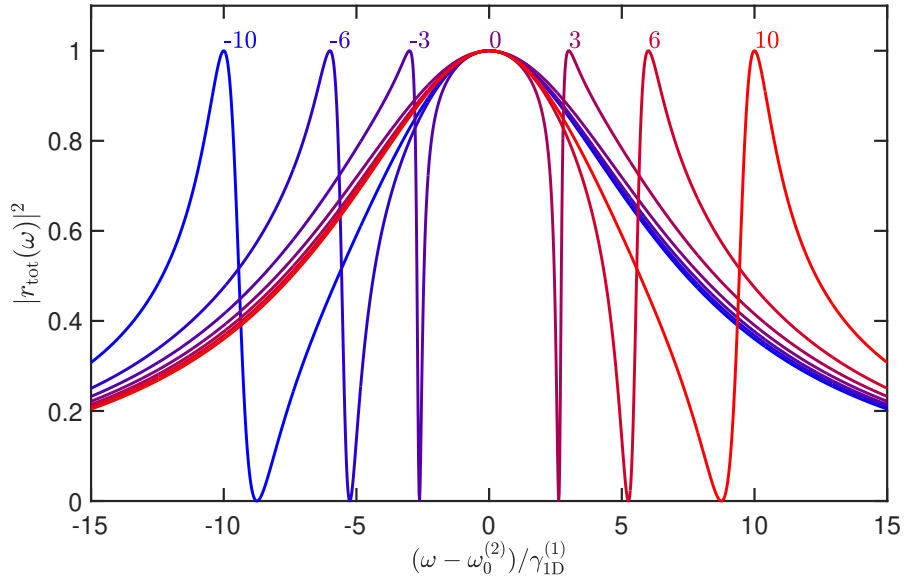

Figure 5.3: Reflection spectra for two unidentical emitters with $\gamma_{\rm 1D}^{(2)} = 7\gamma_{\rm 1D}^{(1)}$. Different curves correspond to different values of $(\omega_0^{(1)} - \omega_0^{(2)})/\gamma_{\rm 1D}^{(1)}$, indicated on graph on top of the curves. Calculation has been performed following Eqs. (9.6) for $\gamma = 0$, $\varphi = 0$.

narrow resonant feature. This feature is, in general, asymmetric and its shape depends on the detuning. Such asymmetric spectral lines are very typical when there exist several resonances with different spectral linewidths in the system and is termed as *Fano resonance*. This follows original work of Ugo Fano on interference of different ionization processes in atomic physics [10] but is now often used in a much broad (maybe, too broad), context. More details on Fano resonances in optical settings can be found in Ref. [11].

5.5 Super- and subradiant modes for $N = 2$

We will now illustrate the non-Hermitian Hamiltonian approach above for two identical coupled emitters . Since their eigenfrequencies will be the same, the interaction effects will be even stronger than in the previous section. They can no longer be treated perturbatively. To find the eigenmodes we will diagonalize of the effective non-Hermitian Hamiltonian matrix Eq. (5.7), that assumes the form

$$H = \begin{pmatrix} \omega_0 - \mathrm{i}(\gamma_{\rm 1D} + \gamma) & -\mathrm{i}\gamma_{\rm 1D}\mathrm{e}^{\mathrm{i}\varphi} \\ -\mathrm{i}\gamma_{\rm 1D}\mathrm{e}^{\mathrm{i}\varphi} & \omega_0 - \mathrm{i}(\gamma_{\rm 1D} + \gamma) \end{pmatrix} . \tag{5.30}$$

We remind that $\varphi = \omega_0 d/c$ is the phase gained by light between the two emitters and plays the role of the dimensionless distance. The eigenfrequencies are given by

$$\omega_\pm = \omega_0 - \mathrm{i}\gamma - \mathrm{i}(\gamma_{1\mathrm{D}} \pm \gamma_{1\mathrm{D}} \mathrm{e}^{\mathrm{i}\varphi}) \,. \tag{5.31}$$

and the eigenvectors correspond to symmetric and antisymmetric excitation, $[1, \pm 1]/\sqrt{2}$. Equations (5.31) show, that both the real and imaginary parts of the two decay rates are renormalized by the interaction:

$$\mathrm{Re}\,\omega_\pm = \omega_0 \pm \gamma_{1\mathrm{D}} \sin\varphi \,, -\mathrm{Im}\,\omega_\pm = \gamma \pm \gamma_{1\mathrm{D}}(1 \pm \cos\varphi) \,. \tag{5.32}$$

Figure 5.4 shows how the real and imaginary parts of the eigenfrequencies depend on the distance between the emitters. Clearly, they exhibit an oscillating behavior. Indeed, the complex off-diagonal terms in Eq. (5.30) have both real and imaginary part. These parts correspond to *dispersive* (also called *exchange*) coupling and *dissipative* coupling, that tend to split real and imaginary parts of the eigenfrequencies, respectively. Such type of oscillating behavior of collective modes has been first observed in Ref. [12] for two trapped ions. Similarly to the case of a single emitter, we interpret the terms $\gamma_{1\mathrm{D}}(1 \pm \cos\varphi)$ as the radiative decay rates of the two coupled emitters. As a sanity check, we see that the decay rates state positive. In other words, $\mathrm{Im}\,\omega_\pm < 0$, which means that the eigenexcitations of the system, $\propto \exp(-\mathrm{i}\omega_\pm t)$, decay in time. The special case, similar to Fig. 5.2 is when $\varphi = 0$ ($\varphi = \pi$). In this case the decay rate for the symmetric (antisymmetric) mode ω_+ (ω_-) is equial to $2\gamma_{1\mathrm{D}}$, twice larger than for an individual emitter. This mode can be called a collective *superradiant* mode of the two emitters: constructive interference between radiation of the two emitters leads to twice large radiative decay rate. The concept of superradiance has been initially put forward by Dicke [13] in a broader context of N emitters and many photon excitations, we will encounter it many times in this book. The antisymetric mode for $\varphi = 0$ (symmetric mode for $\varphi = \pi$) is completely dark, that is, its radiative decay is zero. When the distance between the emitters is changed, and deviates from an exact value of $0, \pi, 2\pi$, the dark states stops being completely dark and becomes subradiant:

$$-\mathrm{Im}\,\omega_- = \gamma + \frac{\varphi^2}{2}\gamma_{1\mathrm{D}} \text{ for } \varphi \ll 1 \,. \tag{5.33}$$

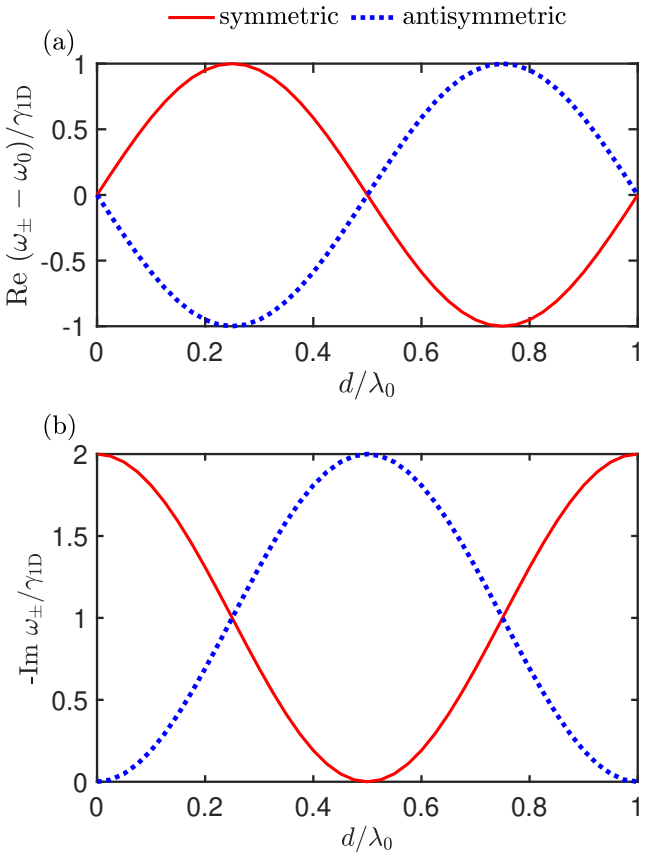

Figure 5.4: Real (a) and imaginary (b) parts of the eigenmodes of two coupled emitters. Calculated following Eqs. (5.31) for $\gamma = 0$.

If the other decay channels are weak $\gamma \ll \gamma_{1D}$, one has $|\operatorname{Im}\omega_-| \ll \gamma_{1D}$ and, according to Eq. (5.22), the mode will be seen as a sharp resonance in the reflection spectrum. It is this subradiant state resonance that is behind the narrow dips in the reflection spectra in Fig. 5.2(a) for φ close to $0, \pi$.

For those more used to quantum mechanics description of the spontaneous emission, there is another simple way to explain collective enhancement or suppression of light emission. Let us use the Fermi Golden rule to calculate the radiative decay rate:

$$-2\operatorname{Im}\omega^{(\nu)} = \frac{2\pi}{\hbar}\int\limits_{-\infty}^{\infty}\frac{\mathrm{d}k}{2\pi}|M_k^{(\nu)}|^2\delta(\hbar\omega_0 - \hbar c|k|) \tag{5.34}$$

Here, M_k is the matrix element for the interaction of the plain electromagnetic wave $\exp(\mathrm{i}kz)$ with the given mode. That, Eq. (5.34) represents the sum of the probabilities of emission of waveguide photons. For simplicity we also in Eq. (5.34) assume $\gamma = 0$. The reason of the factor 2 in the left-hand-side is that the emission rate is twice the imaginary part of the

eigenmode frequency: if $\psi \propto \exp(-\mathrm{i}\omega^{(\nu)}t)$, then $|\psi|^2 \propto \exp(-2\,\mathrm{Im}\,\omega^{(\nu)}t)$. In order to actually use Eq. (5.34) we also need to calculate $M_k^{(\nu)}$. We define it as

$$M_k^{(\nu)} = \hbar g \sum_{m=1}^{N} \mathrm{e}^{\mathrm{i}kdm}\psi_m^{(\nu)}\,, \tag{5.35}$$

where $\hbar g$ is the photon-emitter interaction strength. Since we know that for the two emitters $\psi^{(\pm)} = [1, \pm 1]/\sqrt{2}$ we get

$$M_k^{(\pm)} = \frac{\hbar g}{\sqrt{2}}(1 \pm \mathrm{e}^{\mathrm{i}kd})\,. \tag{5.36}$$

and

$$-2\,\mathrm{Im}\,\omega^{(\nu)} = \frac{2g^2}{c}\left(1 \pm \cos\frac{\omega_0 d}{c}\right)\,. \tag{5.37}$$

If we identify

$$\gamma_{1\mathrm{D}} = g^2/c \tag{5.38}$$

as a spontaneous decay rate of a single emitter in the waveguide, we recover exactly the radiative decay rates from Eq. (5.32).

5.6 Non-Markovian effects

In this section, we will go beyond the Markovian approximation usually used in this book. Namely, we will solve Eq. (5.27) for the collective modes of the two emitters without assuming that they are closed to each other:

$$1 - r^2\exp(2\mathrm{i}\omega d/c) = 0\,. \tag{5.39}$$

Here, we explicitly write $\varphi = \omega d/c$ and we are going to take the dependence of φ on ω into account. For simplicity, we assume both emitters to be the same and we remind that $r = \mathrm{i}\gamma_{1\mathrm{D}}/[\omega_0 - \omega - \mathrm{i}(\gamma + \gamma_{1\mathrm{D}})]$. Substituting explicit expressions for $r(\omega)$ into Eq. (5.39) we find

$$\omega_\pm = \omega_0 - \mathrm{i}\gamma - \mathrm{i}\gamma_{1\mathrm{D}} \mp \mathrm{i}\gamma_{1\mathrm{D}}\exp(\mathrm{i}\omega_\pm d/c)\,. \tag{5.40}$$

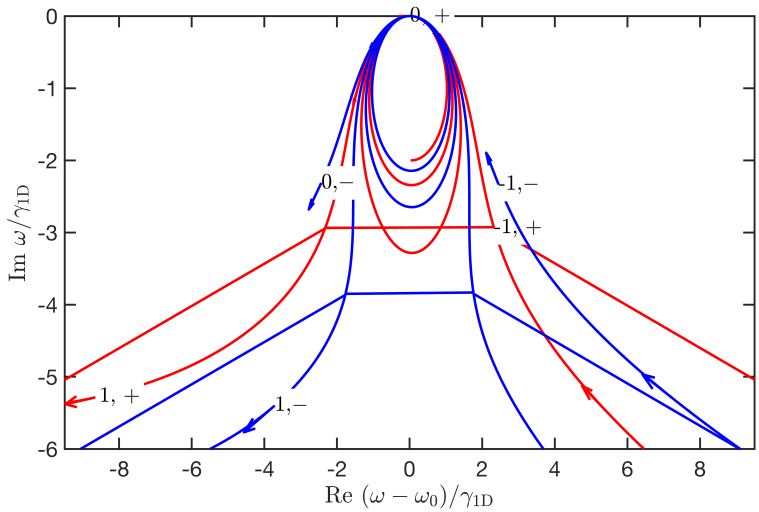

Figure 5.5: Eigenmodes (5.41) of two coupled oscillators beyound the Markovian approximation. Calculated for $\gamma_{1D}/\omega_0 = 0.02, \gamma = 0$ and varying $\omega_0 d/c = 0 \dots 7\pi$. Aarrows indicate the direction of increasing d the values of ν and mode parity sign $\pm$ are indicated near each curve.

Compared to Eq. (5.31), these are now transcendental equations to solve for complex $\omega_\pm$. The solution can be formally written as

$$\omega_\pm^\nu = \tilde{\omega}_0 + \mathrm{i}\frac{c}{d} W_\nu \left[\mp \frac{\gamma_{1D} d}{c} \exp\left(\mathrm{i}\frac{\tilde{\omega}_0 d}{c} \right) \right], \quad \tilde{\omega}_0 \equiv \omega_0 - \mathrm{i}\gamma - \mathrm{i}\gamma_{1D} \,. \tag{5.41}$$

Here, $W_\nu(z)$ is the so-called Lambert W-function, found as solution of $W(z)\exp[W(z)] = z$. Importantly, it is a multibranch function, characterized by the integer index ν. Thus, there are infinite eigenmode solutions for two oscillators! Where do the additional modes come from? The answer is simple — the extra modes are just the Fabry-Pérot modes in the cavity, formed by two emitters, acting as resonant mirrors. There is, in principle, an infinite amount of such modes, so we should not be surprised much. Indeed, at larger $|\nu| \gg z$ the main term in $W_\nu(z)$ asymptotic expression is $2\pi\mathrm{i}\nu$. Being substituted in Eq. (5.41) this gives a set of Fabry Pérot modes separated by $2\pi c/d$.

At small spacing d, when photon flight time d/c is much less than the spontaneous emission lifetime $1/\gamma_{1D}$, the argument of the Lambert functions is small, and one can use the approximate expression $W_0(x) \approx x$. Both solutions of Eq. (5.41) then reduce to

$$\omega_\pm^\nu \approx \tilde{\omega}_0 + \mathrm{i}\frac{c}{d} \left[\mp \frac{\gamma_{1D} d}{c} \exp\left(\mathrm{i}\frac{\tilde{\omega}_0 d}{c} \right) \right] \approx \tilde{\omega}_0 \pm \mathrm{i}\gamma_{1D} \mathrm{e}^{\mathrm{i}\varphi} \,. \tag{5.42}$$

This is equivalent to the usual Markovian approximation answer Eq. (5.31). For $\nu \neq 0$ and

$d \ll c/\gamma_{1D}$ the rest of the solutions will be strongly detuned from ω_0 by the frequency $\sim c/d$.

The complex spectrum of eigenmodes plotted for varying d following Eqs. (5.41) is shown in Fig. 5.5. For low values of d, when $\gamma_{1D}d/c \ll 1$, there only two eigenmodes in the spectra vicinity of the resoance $|\omega - \omega_0| \lesssim \gamma_{1D}$, which are just the usual solutions Eq. (5.31). When the phase $\omega_0 d/c \equiv \varphi$ changes, the imaginary and real parts of these two modes oscillate and they rotate around the point $\omega_0 - \mathrm{i}\gamma_{1D}$, just as shown in Fig. 5.4. This is manifested by spirals in the middle of Fig. 5.5. For large values of d, however, additional Fabry-Pérot modes appear "from infinity" and the eigenspectrum becomes much more complex. Thus, even the seemingly simple problem of two coupled oscillators becomes quite involved beyond the Markovian approximation!

5.7 Summary

To summarize, we have seen that the problem of light scattering on just two emitters is surprisingly rich. The reason behind this is multiple scattering of light from the emitters with constructive or destructive interference. Depending on the distance of the emitters, the difference between their resonant frequencies and their radiative decay rates, one can realize totally different regimes of interaction. The two-emitter problem can illustrate large part of the collective interaction effects. We will however see in the next chapter, that there are also some effects which uncover for larger arrays with $N > 2$.

5.8 Additional reading

Fano-like resonance for cavity side coupled to a waveguide: S. Fan, "Sharp asymmetric line shapes in side-coupled waveguide-cavity systems", Appl. Phys. Lett. **80**, 908 (2002)

Fano resonances in photonics: M. F. Limonov et al., "Fano resonances in photonics", Nat. Photonics **11**, 543–554 (2017).

A detailed discussion of original Purcell work [8] on spontaneous emission: M. Glazov et al., "Purcell Factor in Small Metallic Cavities", Phys. Solid State **53**, 1753 (2011)

Chapter 6

2×2 non-Hermitian Hamiltonian

In the previous chapter, we have seen, that non-Hermitian effective Hamiltonians H_{mn} naturally arise when considering a problem of emitters coupled by light, i.e. by the processes, when photon is emitted by an atom n and reabsorbed by an atom m. The goal of this chapter will be to study the properties of the non-Hermitian Hamiltonians in a bit more detail, without the focus on the particular setup of a one-dimensional emitter array. We will consider the generic situation, where two emitters, that can in principle be different, are coupled to exactly the same electromagnetic mode. This can be realized, for example, when emitters are located in resonance with the same photonic mode of a cavity. As illustrated in Fig. 6.1, this mode will induce both *collective dissipation* for the emitters, when energy is emitted in the far field, and dispersive coupling, when a photon emitted from the first emitter will be reabsorbed by the second one and vice versa.

6.1 Derivation of the Hamiltonian

Let us again rewrite the general equation (5.7) for $N = 2$, assuming that the Green function $G(z_m, z_n) \equiv G$, i.e. it does not depend on the emitter positions. This can be realized when for example emitters are placed close to each other, or in the different antinodes of the standing wave.

$$\begin{pmatrix} \omega_0^{(1)} - a_1 G & -a_1 G \\ a_2 G & \omega_0^{(2)} - a_2 G \end{pmatrix} \begin{pmatrix} p_1 \\ p_2 \end{pmatrix} = \omega \begin{pmatrix} p_1 \\ p_2 \end{pmatrix} . \tag{6.1}$$

Here, we assumed that the only decay mechanism comes from the emission of photons into the mode, so we have set internal decay rates γ to zero. It instructive to symmetrize the problem

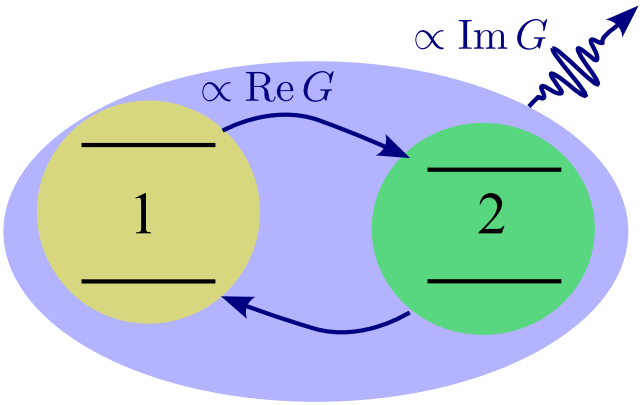

Figure 6.1: Schematic illustration of two emitters coupled to the same electromagnetic enviroment. Real part of the elecrtromagnetic Green function $\mathrm{Re}\, G$ is responsible for the dispersive coupling, imaginary part $\mathrm{Im}\, G$ is responsible for the collective dissipation.

Eq. (6.1) by changing the unknowns to $\psi_{1,2} = p_{1,2}/\sqrt{a_{1,2}}$. For a two-level atom emitters, these amplitudes $\psi_{1,2}$ describe the coherences between the ground and excited states. We also explicitly The system Eq. (6.1) is then transformed to

$$H\psi = \omega\psi, \quad H = \begin{pmatrix} \omega_1 - \mathrm{i}\gamma_1 & g - \mathrm{i}\sqrt{\gamma_1\gamma_2} \\ g - \mathrm{i}\sqrt{\gamma_1\gamma_2} & \omega_2 - \mathrm{i}\gamma_2 \end{pmatrix}, \tag{6.2}$$

where $\omega_{1,2} = \omega_0^{(1,2)} - a_{1,2}\,\mathrm{Re}\, G$ are the resonant frequencies of two coupled emitters (both are real), shifted due to their interaction with photons by $a_{1,2}\,\mathrm{Re}\, G$. The parameter $g = -\sqrt{a_1 a_2}\,\mathrm{Re}\, G$ describes the dispersive part of the coupling and the real parameters $\gamma_{1,2} = -a_{1,2}\,\mathrm{Im}\, G$ describe the dissipation. The form Eq. (6.2) makes the distinction between the dispersive (exchange) and dissipative parts of the effective non-Hermitian Hamiltonian especially clear. We can write

$$H = H_{\mathrm{exch}} + H_{\mathrm{diss}}, H_{\mathrm{exch}} = \begin{pmatrix} \omega_1 & g \\ g & \omega_2 \end{pmatrix}, \quad H_{\mathrm{diss}} = -\mathrm{i} \begin{pmatrix} \sqrt{\gamma_1} \\ \sqrt{\gamma_2} \end{pmatrix} \begin{pmatrix} \sqrt{\gamma_1} \\ \sqrt{\gamma_2} \end{pmatrix}^T. \tag{6.3}$$

The dissipative part is a rank-1 matrix, which is a direct consequence of the fact that the dissipation is due to the emission into a single photonic mode. In a more general case, the number of terms in the expansion of the dissipative part of the effective Hamiltonian is equal to the number of independent decay channels [16].

6.2 Exceptional points. Strong and weak coupling

The eigenfrequencies $\omega_\pm$ of Eq. (6.2) are given by

$$\omega_\pm = \frac{\omega_1+\omega_2}{2} - \mathrm{i}\frac{\gamma_1+\gamma_2}{2} \pm \sqrt{D}, \quad D = \left(\frac{\omega_1-\omega_2-\mathrm{i}\gamma_1+\mathrm{i}\gamma_2}{2}\right)^2 + (g-\mathrm{i}\sqrt{\gamma_1\gamma_2})^2\,. \tag{6.4}$$

Figure 6.2 plots the dependence of the real (a) and imaginary parts (b) of the eigenfrequencies on the dispersive coupling strength g for the case of zero detuning, when $\omega_1 = \omega_2$. We have also chosen $\gamma_2 = 0$, which means that the dissipative part of the coupling matrix element $g - \mathrm{i}\sqrt{\gamma_1\gamma_2}$ in Eq. (6.2) is exactly zero. Even then, the problem is not trivial and there are two qualitatively different coupling regimes. For $|g| < \gamma_1/2 = 1$, the coupling is weaker than the half-difference between the imaginary parts of the complex eigenfrequencies. As a result, the coupling leads to the renormalization of the decay rates, $\mathrm{Im}\,\omega_\pm$ in Fig. 6.2(b), but the real parts stay equal to zero. As a sanity check we see that $\mathrm{Im}\,\omega_\pm < 0$: the eigenexcitations of the system, $\propto \exp(-\mathrm{i}\omega_\pm t)$, decay in time. In the opposite case, $|g| > \gamma_1/2 = 1$, the real parts of the eigenfrequencies are split and imaginary stay the same. This regime of large dispersive coupling is similar to usual avoided crossing of levels in Hermitian problems. In the case when both decay rate and dispersive coupling are present, the parameter range when the coupling is stronger than the decay rates is called strong coupling regimes. It means that the excitations can be coherently transferred between the emitters, and the transfer rate is faster, then the rate of dissipation. The opposite case of small g is called the weak coupling regime. In the very strong coupling regime, one can think of the eigenstates of the non-Hermitian Hamiltonian as hybridized even and odd combinations of the excitations of first and second emitter, $[\psi_1, \psi_2] = [1, \pm 1]/\sqrt{2}$. In the weak coupling regime with $g \ll \gamma_{1,2}$ it is easier to think of the eigenstates as independent modes, $[1, 0]$ and $[0, 1]$.

The transition between the strong and weak coupling regimes goes through the exceptional point, that is seen as square-root singularities in Fig. 6.2 at $g = \pm 1$. Not only two eigenvalues are the same at the exceptional point, but also the eigenvectors coalesce and the Hamiltonian matrix becomes degenerate.

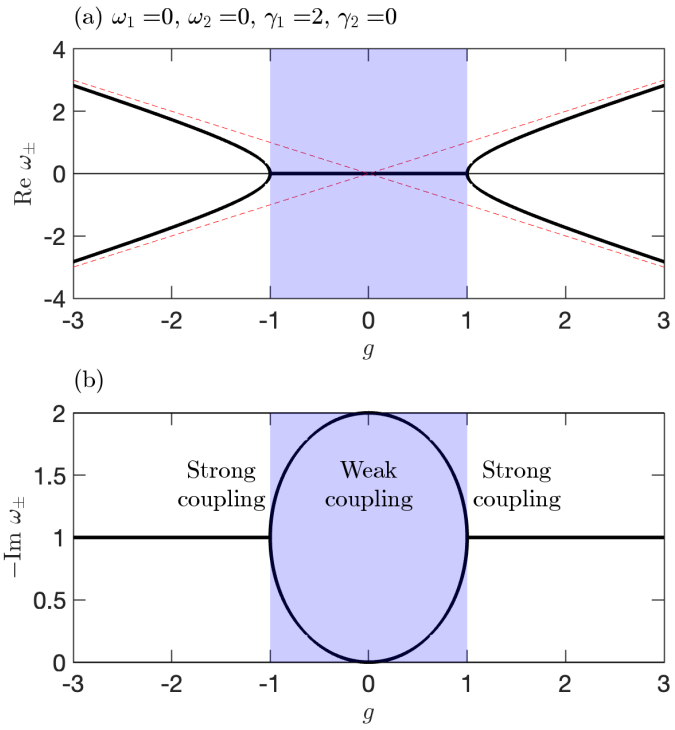

Figure 6.2: Real (a) and imaginary (b) parts of the eigenfrequencies (6.4) depending on the coupling strength g. Calculation has been performed for zero detuning, $\tilde{\omega}_0^{(1)} = \tilde{\omega}_0^{(2)}$ and for $\gamma_2 = 0$. Dashed red lines in (a) show the asymptotic description in the strong dispersive coupling limit, $\omega_\pm = \pm g$. Blue shading indicates the weak coupling regime. Other calculation parameters are indicated on graph.

6.3 Friedrich-Wintgen condition

Figure 6.3 shows the dependence of the complex eigenfrequencies $\omega_\pm$ on g in a slightly more general scenario. Not only the eigenfrequencies ω_1 and ω_2 are detuned from each other, but also $\gamma_2 > 0$, so that there is an extra off-diagonal dissipative coupling term $\sqrt{\gamma_1\gamma_2}$ in Eq. (6.2). One can then see in Fig. 6.3 that there is a special point when one the imaginary part of one of the eigenvalues turns to zero. This point can also be found analytically from Eq. (6.4). If we denote $\sqrt{D} = x + \mathrm{i}y$, we need $y = (\gamma_1 + \gamma_2)/2$ to have real-valued solution. This yields to the condition

$$\mathrm{Re}\, D = x^2 - y^2, \quad \mathrm{Im}\, D = 2xy, \ \text{with } y = \frac{\gamma_1 + \gamma_2}{2}\,. \tag{6.5}$$

Finding x from the first equation and substituting in the second one, we find

$$\mathrm{Re}\, D - (x^2 - y^2) \propto \left(g - \frac{\sqrt{\gamma_1\gamma_2}(\omega_1 - \omega_2)}{\gamma_1 - \gamma_2}\right)^2 \tag{6.6}$$

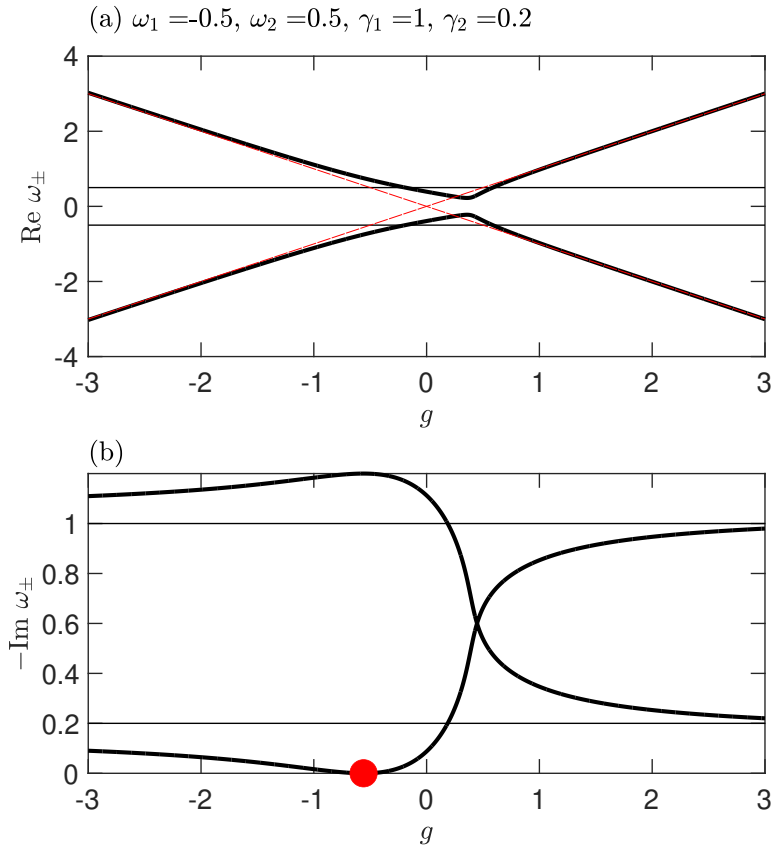

Figure 6.3: Real (a) and imaginary (b) parts of the eigenfrequencies (6.4) depending on the coupling strength g. Calculation has been performed in the detuned case, $|\tilde{\omega}_0^{(1)} - \tilde{\omega}_0^{(2)}| = 1$. Red dot indicates the Friedrich-Wintgen condition Eq. (6.7), where the imaginary part of one of the eigenmodes is exactly zero. Dashed red lines in (a) show the asymptotic description in the strong dispersive coupling limit, $\omega_\pm = \pm g$. Thin horizontal lines show the eigenfrequencies assuming no coupling between the emitters. Other calculation parameters are indicated on graph.

which leads to

$$\sqrt{\gamma_1\gamma_2}(\omega_1 - \omega_2) = g(\gamma_1 - \gamma_2)\,. \tag{6.7}$$

This is a so-called Friedrich-Wintgen condition, named after the authors of Ref. [17]. Currently, it is often used in the context of so-called bound states in continuum in photonic structures [18], where it describes destructive interference of decay via two different decay channels. In the previous chapter, discussing two emitters coupled to the same waveguide mode, we have already encountered such points with $\mathrm{Im}\,\omega_\pm = 0$ and associated them with dark states see Fig. 5.4 for $d = 0, \lambda/2, \lambda$. There we considered identical emitters with no detuning, $\omega_1 = \omega_2$ and $\gamma_1 = \gamma_2$. The The Friedrich-Wintgen condition then reduces to just $g = 0$, zero dispersive coupling. This is exactly the case for $d = 0, \lambda/2, \lambda$, when the Green function $\propto \mathrm{i}\exp(2\pi\mathrm{i}\varphi) \equiv \mathrm{i}\exp(2\pi\mathrm{i}d/\lambda)$ is purely imaginary. Thus, the dark states present a particular realization of the Friedrich-Wintgen

condition.

6.4 Summary

To summarize, in this chapter, we have learned that even the seemingly simple problem of two emitters coupled to the same electromagnetic environment can be nontrivial. Depending on the spectral detuning between the emitter resonances, their decay rates, and the dispersive coupling strength, one can realize both strong coupling regimes when excitations of both emitters can be hybridized by hopping from one emitter to another and back, and the weak coupling regimes, when the excitations dissipate faster than hopping and thus stay localized. Transitions between the two regimes goes through exceptional points. There are also special cases, when the decay rate of one of the modes becomes exactly zero, i.e. the mode is dark and does not dissipate in the environment.

6.5 Additional reading

More on symmetry of 2×2 non-Hermitian Hamiltonians in optics [19] .

Discussion of non-Hermitian Hamiltonian for a general system: W. Suh et al., "Temporal coupled-mode theory and the presence of non-orthogonal modes in lossless multimode cavities", IEEE Journal of Quantum Electronics **40**, 1511–1518 (2004) .

Chapter 7

Light interaction with $N > 2$ periodically spaced emitters.

The goal of this chapter will be to study the collective light interaction with $N > 2$ emitters, arranged in the periodic array and coupled to the waveguide mode, see Fig. **??**. Some of the phenomena, such as formation of collective super- and sub-radiant eigenmodes, will be essentially the same as in the case of $N = 2$. The super-radiant modes will just get brighter, and the subradiant modes will just be darker for a larger number of emitters N. However, there will be also new phenomena for long periodic arrays. We will show, that light can see a long periodic array of emitters either as an effective medium, where the interaction will be averaged over all the emitters, or as a resonant periodic photonic crystal. In the first case the whole array can be described by some effective permittivity, in the second case, the photonic *band gap* will form, similarly to band gaps for electrons in usual crystals. The description of such interaction of light with arrays will require different theoretical tools.

7.1 Collective super- and subradiant modes for N emitters.

Let us again look for the eigenstates Eq. (5.7) in the case of the periodic array, when $\omega_0 z_m/c \equiv \varphi m$, and $\varphi = \omega_0 d/c$ is still the phase gained by light between the two emitters.

$$\omega_0 p_m - \mathrm{i}\gamma_{1\mathrm{D}} \sum_{n=1}^{N} \mathrm{e}^{\mathrm{i}\varphi|m-n|} p_n = \omega p_m, \quad m = 1, 2 \ldots N, \tag{7.1}$$

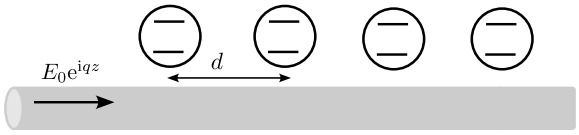

Figure 7.1: Periodic array of resonant scatterers coupled to the waveguide.

where $varpi = 2\pi d/\lambda$ is the phase gained by light propagating between the two neighboring emitters. In this chapter, we will focus on specific case of the Bragg-spaced array. when $d = \lambda/2$, so $\varphi = \pi$.

We start by rewriting the coupled equations using the fact that $\varphi = \pi$:

$$\omega_0 p_m - \mathrm{i}\gamma_{1\mathrm{D}} \sum_{n=1}^{N} (-1)^{m+n} p_n = \omega p_m, \quad m = 1, 2 \ldots N, \tag{7.2}$$

Next, we make the substitute $(-1)^m p_m = \chi_m$ which leads to

$$\omega_0 \chi_m - \mathrm{i}\gamma_{1\mathrm{D}} \sum_{n=1}^{N} \chi_n \equiv -\mathrm{i}\gamma_{1\mathrm{D}} \Lambda = \omega \chi_m, \quad m = 1, 2 \ldots N, \quad \Lambda = \sum_{n=1}^{N} \chi_n \,. \tag{7.3}$$

The same equations describe the systems with $d = 0, \lambda, 2\lambda \ldots$. Next, we can sum the equation (7.3) over m:

$$(\omega + \mathrm{i}\gamma_{1\mathrm{D}} N - \omega_0)\Lambda = 0 \,. \tag{7.4}$$

From this we find that if $\Lambda \neq 0$ than $\omega = \omega_0 - \mathrm{i}\gamma_{1\mathrm{D}} N$. For the solution with $\omega = \omega_0 - \mathrm{i}\gamma_{1\mathrm{D}} N$ we find from Eq. (7.3) that all χ_m are the same. For the solution with $\Lambda = 0$ Eq. (7.3) means that $\omega = 0$.

Hence, there is a symmetric solution with

$$\chi_1 = \chi_2 = \ldots \chi_N, \omega = \omega_0 - \mathrm{i} N \gamma_{1\mathrm{D}} \tag{7.5}$$

and $N - 1$ states with $\omega = \omega_0$, where eigenvectors satisfying the condition

$$\sum_{n=1}^{N} \chi_n = 0, \omega = \omega_0 \,. \tag{7.6}$$

The first solution demonstrates collective enhancement of the spontaneous emission rate, $-\operatorname{Im}\omega = N\gamma_{1\mathrm{D}}$, it is a Dicke superradiant mode. The radiative decay rate for this mode grows

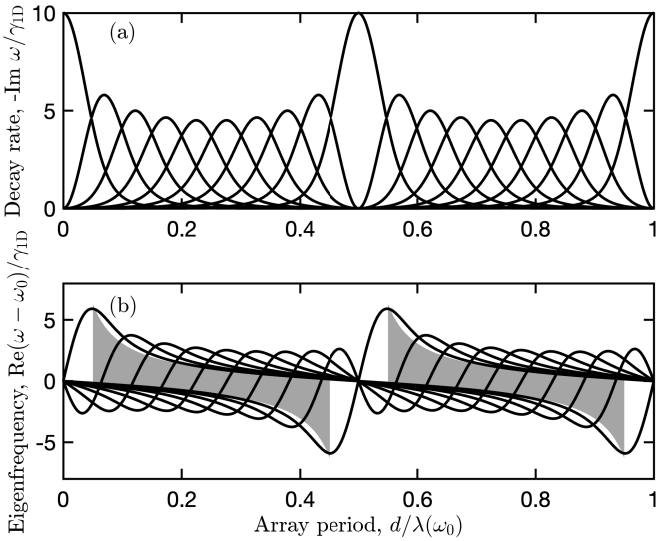

Figure 7.2: From Ref. [20]. Imaginary (a) and real (b) parts of the complex eigenfrequencies of the array of $N = 10$ atoms coupled to a waveguide depending on the period of the array d. Shaded areas (b) show the edges of the polariton band gaps. Each value of d/λ corresponds to $N = 10$ eigenvalues.

proportionally to the number of emitters. This is the most basic effect of collective dissipative interaction. All the other modes have zero decay rates, and can be termed as dark. These super- and sub-radiant modes can be seen as generalization of the modes (5.32) for $N = 2$ emitters for the particular case of $\varphi = \pi$.

Let us now consider a more general case of arbitrary spacing. We plot in Fig. 7.2 the complex eigenfrequencies of Eq. (7.2) for $N = 10$. As already expected after considering the two-emitter case, the eigenfrequencies oscillate with the array period d. At $d = 0, \lambda_0/2, \lambda_0$ there is one superradian state and $N - 1$ dark states. When the period is detuned from this condition, the dark states acquire nonzero decay rate.

How does this picture depend on N? For the superradiant state, the answer is already known and trivial, $\omega = \omega_0 - \mathrm{i}N\gamma_{1D}$. The scaling of the decay rates for subradiant states can be found using the Fermi Golden rule, similarly to the case of $N = 2$ emitters, considered in Sec. 5.5:

$$-2\,\mathrm{Im}\,\omega = 2\pi \int_{-\infty}^{\infty} \frac{\mathrm{d}k}{2\pi} |M_k|^2 \delta(\omega_0 - c|k|), \quad M_k = g \sum_{m=1}^{N} \mathrm{e}^{\mathrm{i}kdm} \psi_m \,. \tag{7.7}$$

Here, M_k is the matrix element of the interaction of the state ψ_m with photon with wave vector k , ω_0 is the emitter resonance frequency, d is the array period, g is the coupling constant. We

Figure 7.3: Schematics of the spatial profile of the most superradiant (left) and most subradiant modes (right).

can also rewrite the decay rate as

$$-2\,\mathrm{Im}\,\omega = \frac{1}{c}M_0^2, \quad M_0 = g\sum_{m=1}^{N} \mathrm{e}^{\mathrm{i}\varphi m}\psi_m\,, \varphi = \omega_0 d/c\,. \tag{7.8}$$

Let us now calculate the decay rate for the states with

$$\psi_m = \frac{1}{\sqrt{N}} \quad \text{(superradiant state)}\,, \tag{7.9}$$

$$\psi_m = \sqrt{\frac{2}{N}}(-1)^m \sin\frac{\pi(m-1/2)}{N} \quad \text{(most subradiant state for } \omega_0 d/c \ll 1) \tag{7.10}$$

Here, we assume that $N \gg 1$. The states are illustrated in the Fig. 7.3. We have already proved that Eq. (7.9) is the eigenstate. We give here Eq. (7.10) for the subradiant state without proof. The derivation can be found in Ref. [21] and it can be also easily checked numerically that is the darkest state. It is also easy to see that Eq. (7.10) satisfies the condition $\sum_{m=1}^{N}\psi_m = 0$. The sign oscillations lead to the destructive interference of the photon emission from different emitters and suppress the overall decay rate. For the Dicke superradiant state, the decay rate calculation is trivial and yields $M_0 = g\sqrt{N}$ and $-2\,\mathrm{Im}\,\omega = 2N\gamma_{1\mathrm{D}}$. As expected, the radiative decay rate is enhanced $\propto N$ because of the constructive interference of the waves from different emitters.

For the subradiant states, the calculation is more involved. We first find

$$M_0 = -\frac{\sqrt{2}\left(\mathrm{e}^{i\varphi} + \mathrm{e}^{\mathrm{i}\varphi(N+1)} - \mathrm{e}^{\mathrm{i}N\varphi} - 1\right)}{\sqrt{N}\left(\mathrm{e}^{2\mathrm{i}\varphi} + 2\cos\frac{\pi}{N}\mathrm{e}^{\mathrm{i}\varphi} + 1\right)}\sin\frac{\pi}{2N} \tag{7.11}$$

and then expand this up to the linear terms φ to find

$$M_0 = -\frac{\mathrm{i}g\sqrt{2}\varphi}{4N^{3/2}}\,, \tag{7.12}$$

which results in

$$-2\,\mathrm{Im}\,\omega = \frac{\pi^2(\omega_0 d/c)^2}{8N^3}\gamma_{1\mathrm{D}}\ \text{(most subradiant state)}\,, \tag{7.13}$$

where $\gamma_{1\mathrm{D}} = g^2/c$. This answer can also be found in [21]. It means that the state quickly becomes darker for larger N. It has been proved in Ref. [22] that such $1/N^3$ scaling is universal. The reason for such quick suppression can be intuitively understood as follows. First, the state Eq. (7.10) oscillates with a π-phase difference between neighboring sites, which suppresses the light-matter coupling matrix element M_0. Second, it is also close to zero at the border of the structure, see Fig. 7.3. Since the radiative decay goes through the edges of the array, this state kind of stays away from the edges, which gives an extra power of N in denominator. One can quickly check this by calculating the decay rate for example for a simpler trial function of $\psi_n = (-1)^n/\sqrt{N}$, that will be parametrically larger. In special cases the decay rate can decrease with N even faster, see review [20] and references therein.

7.2 Transfer matrix method

7.2.1 General approach

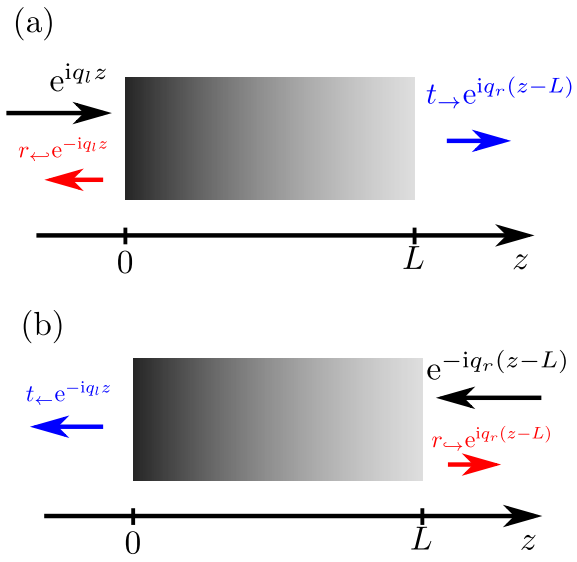

Figure 7.4: Definition of reflection coefficients $r_{\hookleftarrow}$, $r_{\hookrightarrow}$ and transmission coefficients $t_{\rightarrow}$, $t_{\leftarrow}$ of light, incident upon the scatterer with length L from left (a) and right (b) half-spaces, respectively.

We consider one-dimensional problem of light scattering on a general object, see Fig. 7.4. The scattering is characterized by the transfer matrix T that can be conveniently expressed in

the basis of right-propagating (E^+) and left-propagating (E^-) waves

$$E(z) = \begin{cases} E^+_{\text{left}} e^{iq_l z} + E^-_{\text{left}} e^{-iq_l z} & (z < 0) \\ E^+_{\text{right}} e^{iq_r (z-L)} + E^-_{\text{right}} e^{-iq_r (z-L)} & (z > L)\,, \end{cases} \tag{7.14}$$

where $q_{r,l}$ are light wave vectors from the left and from the right of the scatterer. The 2×2 matrix T relates the electric field amplitudes by

$$\begin{pmatrix} E^+_{\text{right}} \\ E^-_{\text{right}} \end{pmatrix} = T \begin{pmatrix} E^+_{\text{left}} \\ E^-_{\text{left}} \end{pmatrix} . \tag{7.15}$$

Goal: Express the transfer matrix elements via the complex reflection coefficients $r_{\hookleftarrow}$, $r_{\hookrightarrow}$ and transmission coefficients $t_{\rightarrow}$, $t_{\rightarrow}$ corresponding to the initial wave incidence from the left and right sides, as illustrated in Fig. 7.4.

Answer:

$$T = \frac{1}{t_{\rightarrow}} \begin{pmatrix} t_{\rightarrow} t_{\rightarrow} - r_{\hookleftarrow} r_{\hookrightarrow} & r_{\hookrightarrow} \\ -r_{\hookleftarrow} & 1 \end{pmatrix} . \tag{7.16}$$

It can be proved that this is indeed an answer by checking the relations

$$T \begin{pmatrix} 1 \\ r_{\hookleftarrow} \end{pmatrix} = \begin{pmatrix} t_{\rightarrow} \\ 0 \end{pmatrix}, \quad T \begin{pmatrix} 0 \\ t_{\rightarrow} \end{pmatrix} = \begin{pmatrix} r_{\hookrightarrow} \\ 1 \end{pmatrix} . \tag{7.17}$$

for scattering of the the waves incident from the left and from the right.

$$T_{\text{tot}} = T_N T_{N-1} \ldots T_2 T_1 \tag{7.18}$$

$$r_{\hookleftarrow} = -\frac{T_{2,1}}{T_{2,2}}, \quad t_{\rightarrow} = \frac{\det T}{T_{2,2}} \tag{7.19}$$

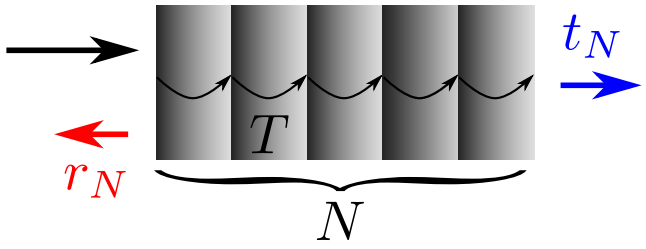

Figure 7.5: Schematics of light reflection and transmission from a structure with N scatterers.

7.2.2 Reflection and transmission from a periodic structure

We consider light reflection from a periodic structure containing N unit cells, see Fig. 7.5. The transfer matrix through 1 unit cell is given be

$$T = \frac{1}{t_1}\begin{pmatrix} t_1^2 - r_1^2 & r_1 \\ -r_1 & 1 \end{pmatrix} . \tag{7.20}$$

Goal: Calculation reflection coefficients r_N and t_N for the structure. Express them via r_1, t_1 and the eigenvalues of the transfer matrix $\exp(\pm \mathrm{i}K)$.

Answer:

$$r_N = \frac{r_1 \sin(NK)}{\sin(NK) - t_1 \sin[(N-1)K]} \, , t_N = \frac{t_1 \sin K}{\sin(NK) - t_1 \sin[(N-1)K]} \, , \tag{7.21}$$

Solution: The solution can be found e.g. in [23] and [24], see also [**yariv**].

To find the solution we first find the eigenvectors of the transfer matrix $C_{1,2}$ that are defined as $TC_{1,2} = \mathrm{e}^{\pm \mathrm{i}K} C_{1,2}$. Using the explicit transfer matrix definition we find

$$C_{1,2} = \begin{pmatrix} 1 \\ a_{1,2} \end{pmatrix} , \quad a_{1,2} = \frac{r}{1 - t\mathrm{e}^{\pm \mathrm{i}K}} \, . \tag{7.22}$$

Next, we use the boundary conditions. On the left of the structure, the field amplitudes are given by $E_L = \left(\begin{smallmatrix} 1 \\ r_N \end{smallmatrix}\right)$ and on the right side the field amplitudes are $E_R = \left(\begin{smallmatrix} t_N \\ 0 \end{smallmatrix}\right)$. The transfer matrix connects fields on the left and on the right

$$T^N E_L = E_R \, . \tag{7.23}$$

In order to calculate T^N we expand the electric field in terms of the eigenvectors $C_{1,2}$,

$$E_L = C_1 f_1 + C_2 f_2, \quad f_1 = -\frac{a_2 - r_N}{a_1 - a_2}, \quad f_2 = \frac{a_1 - r_N}{a_1 - a_2} \,. \tag{7.24}$$

Next, we can write

$$E_R = T^N E_L = C_1 \mathrm{e}^{\mathrm{i}KN} f_1 + C_2 \mathrm{e}^{-\mathrm{i}KN} f_2 \,. \tag{7.25}$$

Since $E_R = \binom{t_N}{0}$ we find

$$f_1 = -\frac{a_2 t_N \mathrm{e}^{-\mathrm{i}KN}}{a_1 - a_2}, \quad f_2 = \frac{a_1 t_N \mathrm{e}^{\mathrm{i}KN}}{a_1 - a_2} \,. \tag{7.26}$$

Combining Eq. (7.26) and Eq. (7.24) and solving them for r_N, t_N we obtain Eqs. (7.21).

7.3 Polariton dispersion

We consider wave propagation in a one-dimensional periodic array of scatterers, shown in Fig. 7.1. Wave scattering on each period is characterized by the 2×2 transfer matrix

$$T = T_{\text{free}} T_{\text{res}} \tag{7.27}$$

where

$$T_{\text{free}} = \begin{pmatrix} \mathrm{e}^{\mathrm{i}qd} & 0 \\ 0 & \mathrm{e}^{-\mathrm{i}qd} \end{pmatrix} \tag{7.28}$$

is the transfer matrix for the free waveguide propagation in the basis of propagating waves, $q = \omega/c$, and

$$T_{\text{res}} = \frac{1}{t} \begin{pmatrix} t^2 - r^2 & r \\ -r & 1 \end{pmatrix}, \quad r = \frac{\mathrm{i}\gamma_{1\mathrm{D}}}{\omega_0 - \omega - \mathrm{i}(\gamma_{1\mathrm{D}} + \gamma)}, \quad t = 1 + r. \tag{7.29}$$

is the resonant matrix of a scatterer.

We are interested in the propagating Floquet-Bloch solutions, that satisfy $T\psi = \mathrm{e}^{\mathrm{i}K}\psi$.

Goal: Find the dispersion equation, that is express $\cos K$ via the transfer matrix elements.

Answer: We use the general answer $\cos K = \operatorname{Tr} T/2$ and find

$$\cos K = \cos qd - \frac{\sin qd\gamma_{1\mathrm{D}}}{\omega_0 - \omega - \mathrm{i}\gamma} \,. \tag{7.30}$$

This answer has been obtained in [25] for the array of quantum wells.

We are interested in finding the eigenstate ψ and the eigenfrequency ω for the infinite array of emitters:

$$\sum_{n=-\infty}^{\infty} H_{m,n}\psi_n = \omega\psi_m, \quad H_{m,n} = (\omega_0 - \mathrm{i}\gamma)\delta_{mn} - \mathrm{i}\gamma_{1\mathrm{D}}\mathrm{e}^{\mathrm{i}\omega_0 d|m-n|/c}\,. \tag{7.31}$$

Here, ω_0 is the resonant frequency, c is the speed of light, γ is the nonradiative decay rate, $\gamma_{1\mathrm{D}}$ is the radiative decay rate. Due to the translational symmetry of the problem, $H_{m+l,n+l} = H_{m,n}$ the solution ψ_m can be sought in the form

$$\psi_m = \psi_0\mathrm{e}^{\mathrm{i}Km}, \tag{7.32}$$

where K is the polariton wave vector depeding on ω.

Goal: substitute Eq. (7.32) into Eq. (7.31) and find the equation for $K(\omega)$ describing the law $\omega(K)$. Plot $K(\omega)$ numerically in the range $\omega_0 - 10\gamma_{1\mathrm{D}} < \omega < \omega_0 + 10\gamma_{1\mathrm{D}}$ for the following set of parameters: $\gamma = 0, \omega_0 d/c = 0.5$.

Answer:

$$\cos K = \cos\tfrac{\omega_0 d}{c} - \frac{\gamma_{1\mathrm{D}}\sin\frac{\omega_0 d}{c}}{\omega_0 - \omega - \mathrm{i}\gamma}\,. \tag{7.33}$$

7.4 Effective-medium approximation

Goal: Simplify the dispersion law in the limit $K \ll 1$, $\omega d/c \ll 1$ and rewrite it in the form $K^2 = \omega^2\varepsilon_{\mathrm{eff}}(\omega)/c^2$. Obtain the expression for the effective medium permittivity $\varepsilon_{\mathrm{eff}}(\omega)$. Plot on the same plot the dispersion law obtained exactly and in the effective medium approximation for $\omega_0 d/c = 0.5\pi$ and $\omega_0 d/c = 0.97\pi$ (take $\gamma_{1\mathrm{D}}/\omega_0 = 10^{-2}$).

Answer:

$$\varepsilon_{\mathrm{eff}}(\omega) = 1 + \frac{2\gamma_{1\mathrm{D}}}{\omega d/c(\omega_0 - \omega)}\,. \tag{7.34}$$

The dispersion law is plotted in Fig. 7.7. It shows avoided crossing between the emitter resonance, $\omega = \omega_0$ and the light dispersion without emitter $\omega = cK$ (thin lines). Surprisingly, the effective medium approximation works well even for a large period $\omega_0 d/c = 0.5\pi$. For a

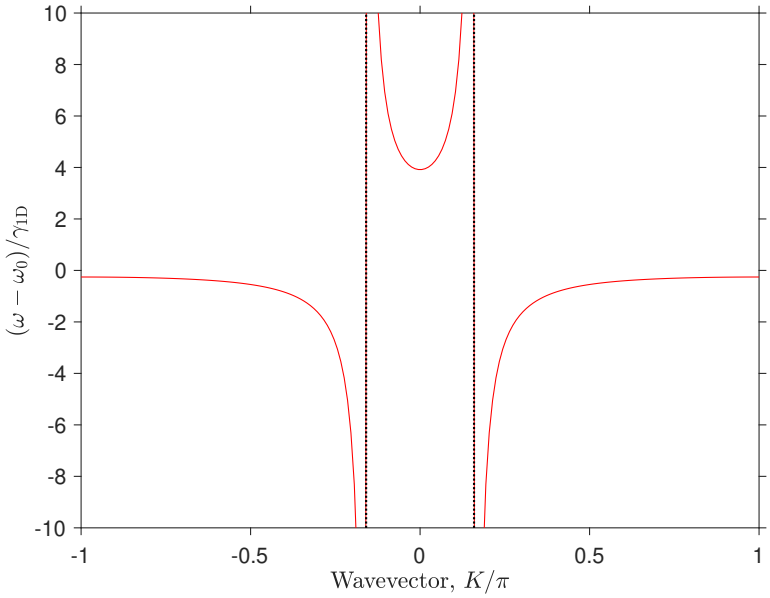

Figure 7.6: Dispersion law in the array of emitters. Calculation has been performed for $\varphi = 0.15\pi$.

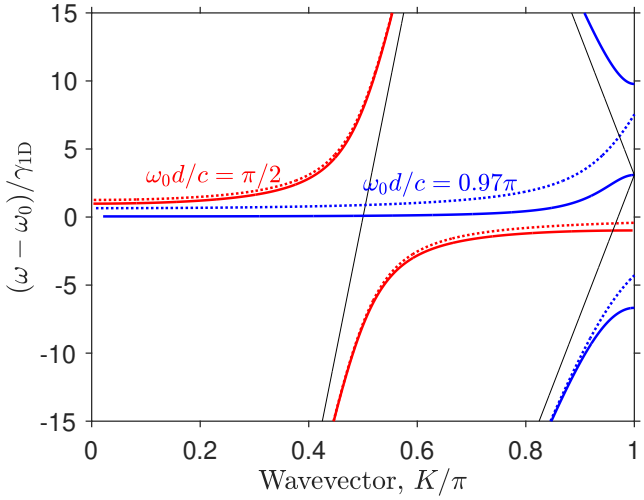

Figure 7.7: Dispersion law in the array of emitters.

close-to-Bragg period , $\omega_0 d/c = 0.97\pi$, there is an additional band gap in the dispersion.

$$|t_N(\omega)|^2 = \mathrm{e}^{-\mathrm{OD}}, \quad \mathrm{OD} = \frac{2N\gamma\gamma_{1D}}{(\omega - \omega_0)^2 + \gamma^2}\,. \tag{7.35}$$

7.5 Bragg-spaced arrays

Blue lines show the edges of the photonic band gaps found from the condition $\mathrm{Im}\, K = 0$. Clearly, the reflection coefficient is at maximum inside the band gaps.

The situation when the atomic resonance frequency and array period d satisfy the resonant

Appendix A

Green function for the Helmholtz equation

Here we will find the Green function $G(z)$ of the one-dimensional Helmholtz equation , satisfying the equation

$$\frac{\mathrm{d}^2 G(z)}{\mathrm{d}z^2} + q^2 G(z) = -4\pi q^2 \delta(z)\,. \tag{A.1}$$

where $q = \omega/c$ is the light wavevector. At $z \to \pm\infty$, the Green function should describe the outgoing wave, that is, it should satisfy the radiating boundary conditions.

We first note that for $z > 0$ or $(z < 0)$ the right-hand side of Eq. (A.1) is zero. Hence, we can choose the Green function in the form of plane waves, that satisfy the homogeneous wave equation:

$$G(z) = \begin{cases} A_+ \mathrm{e}^{\mathrm{i}qz} + A_- \mathrm{e}^{-\mathrm{i}qz}, & (z > 0) \\ B_+ \mathrm{e}^{\mathrm{i}qz} + B_- \mathrm{e}^{-\mathrm{i}qz}, & (z < 0)\,. \end{cases} \tag{A.2}$$

We also use the radiation boundary conditions $A_- = 0$ and $B_+ = 0$, that is we assume that the answer can not contain any terms corresponding to the waves incident on the source, only the terms propagating from the source. Due to mirror symmetry of the original equation $A_+ = B_- \equiv A$ and the Green function can be sought as

$$G(z) = \begin{cases} A\mathrm{e}^{\mathrm{i}qz}, & (z > 0) \\ A\mathrm{e}^{-\mathrm{i}qz} (z < 0)\,. \end{cases} \equiv A\mathrm{e}^{\mathrm{i}q|z|}\,. \tag{A.3}$$

Now we need to satisfy the equation also at $z = 0$, that is, to find A. To this end, we can

formally substitute the expression $A\mathrm{e}^{\mathrm{i}q|z|}$ in the left-hand side. Using the identities

$$\frac{\mathrm{d}}{\mathrm{d}z}|z| = \operatorname{sign} z, \quad \frac{\mathrm{d}}{\mathrm{d}z}\operatorname{sign} z = 2\delta(z) \tag{A.4}$$

we find that

$$\frac{\mathrm{d}^2 G(z)}{\mathrm{d}z^2} + q^2 G(z) = 2\mathrm{i}qA\delta(z) \tag{A.5}$$

which results in the answer

$$G(z) = 2\pi\mathrm{i}q\mathrm{e}^{\mathrm{i}q|z|}\,. \tag{A.6}$$

Appendix B

Resonant susceptibility

Here, we provide more intuition intro Eq. (4.6) for the resonant emitter susceptibility. Let us consider a toy model for an atom interacting with the electric field. The model represents a charge q with mass m moving in a harmonic potential $m\omega_0^2 z^2/2$ with the resonance frequency ω_0 around a charge $-q$. The moving charge then satisfies the Newton equation of motion

$$m\ddot{z} - 2m\gamma\dot{z} + m\omega_0^2 z = q[E(z)\mathrm{e}^{-\mathrm{i}\omega t} + E^*(z)\mathrm{e}^{\mathrm{i}\omega t}]\,, \tag{B.1}$$

where the right-hand side is the force acting upon the atom because of the time-dependent electromagnetic field $E(z,t) = E(z)\mathrm{e}^{-\mathrm{i}\omega t} + E^*(z)\mathrm{e}^{\mathrm{i}\omega t}$. We have also introduced a phenomenological friction force described by the coefficient γ. The dipole moment of the atom is given by $p_{\mathrm{tot}} = qz(t)$ and can be sought in the form $p_{\mathrm{tot}}(t) = p\exp[-\mathrm{i}\omega t] + c.c.$ Solving Eq. (B.1) for $p(t) \propto \mathrm{e}^{-\mathrm{i}\omega t}$ we find

$$p = \alpha E, \quad \alpha = \frac{q^2}{m[\omega_0^2 - \omega^2 - 2\mathrm{i}\omega\gamma]}. \tag{B.2}$$

It is easy to show that for $\gamma \ll \omega_0$ Eq. (B.2) becomes equivalent to Eq. (4.6) with $a = q^2/(m\omega_0)$.